



Escola Tècnica Superior d'Enginyeria  
de Telecomunicació de Barcelona

UNIVERSITAT POLITÈCNICA DE CATALUNYA

# PROJECTE FINAL DE CARRERA

Simulador de comunicacions òptiques

Optical communications simulator

*Estudis: Enginyeria de Telecomunicació*

*Autor: David Safont Cervera*

*Director/a: Joan M. Gené Bernaus*

*Any: 2013*



## Index

Abstract .....	3
Chapter 1 Introduction.....	4
1.1. General simulation concepts.....	4
1.2. Signal model .....	6
Chapter 2 Devices .....	7
2.1. Optical fiber.....	7
2.1.1. Attenuation in optical fibers.....	7
2.1.2. Dispersion in optical fibers.....	8
2.1.3. Mathematical model .....	10
2.2. Photodetector PIN.....	11
2.2.1. Working principle .....	11
2.2.2. Parameters .....	12
2.2.3. Mathematical model .....	13
2.3. X coupler.....	15
2.4. Interferometer .....	16
2.5. Mach Zender Modulator (MZM) .....	17
2.5.1. Working principle .....	17
2.5.2. Mathematical model .....	18
2.5.3. Drive configuration.....	21
2.5.4. Pulse carver .....	23
2.6. Optical Filters .....	26
2.6.1. Raised cosine filter .....	26
2.6.2. Gaussian filter.....	27
Chapter 3 Optical Modulations.....	29
3.1. Intensity Modulation.....	29
3.1.1. Transmitter OOK .....	29
3.1.2. Receiver OOK.....	31
3.3. Phase Modulation .....	32
3.3.1. Transmitter BPSK.....	32

3.3.2.	Receiver BPSK.....	34
3.3.3.	Transmitter QPSK .....	36
3.3.4.	Receiver DQPSK.....	39
Chapter 4	BER.....	43
4.1.	Introduction .....	43
4.2.	Estimation methods .....	44
4.2.1.	Monte Carlo.....	44
4.2.2.	Analytic.....	45
4.2.3.	Semi-Analytic.....	45
Chapter 5	Simulation Examples .....	46
5.1.	Simulation 1.....	46
5.2.	Simulation 2.....	50
5.3.	Simulation 3.....	52
References.....		54

# Abstract

The scope of this project is to design a general optical communications simulator with matlab. A signal model, including polarization states, is defined, and then several mathematical models are built in order to perform some basic simulations.

The modulations considered in this project are just the most basic ones: OOK, BPSK and QPSK. So as to be able to make simulations, it is needed the models for the transmitter and receiver, and also for the optical fiber and optical amplifiers.

So, in summary, all the elements to perform simple simulations are considered, designed and implemented through mathematical models in order to calculate some useful parameters in communication systems like BER, and eye-diagrams.

# Chapter 1 Introduction

## 1.1. General simulation concepts

There are several concepts that should be clarified when simulating communication systems. One of them is the relationship between the time window and the frequency bandwidth. In fact, the bandwidth is inversely proportional to the bit time, as shown in the figure below:

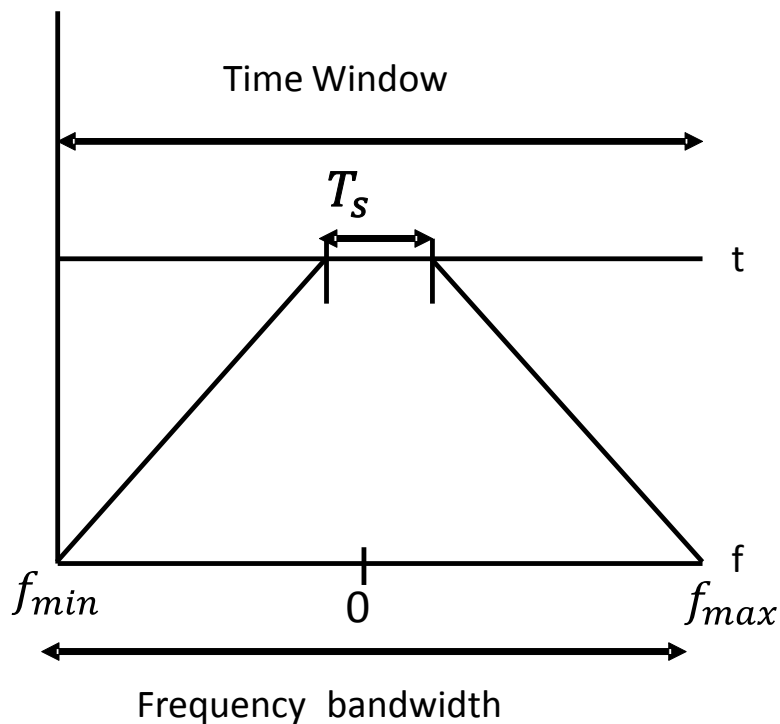


**Figure 1.1-1. Relationship time-frequency in simulations**

In order to perform a simulation, the signals must be sampled. So the signal will be defined as a stream of bits, each one of them will be represented with a determined number of samples. Therefore, the number of points considered in the simulation is:

**Eq. 1.1-1**

$$n_p = (\text{Samples/Bit}) * n$$

Where  $n$  is the number of bits.

Another important parameter of a digital communications signal is the symbol rate ( $R_s$ ), which altogether with the samples per bit, determine the sample rate ( $f_R$ ):

**Eq. 1.1-2**

$$f_R = R_s * (\text{Samples/Bit})$$

The time window is also related with the parameters commented above. This relationship can be written as:

**Eq. 1.1-3**

$$TW = n * R_s$$

## 1.2. Signal model

The signal model used in this simulator is composed by the addition of the signal samples and the polarization parameters. A general expression for representing a communications signal and its polarization state is shown in **¡Error! No se encuentra el origen de la referencia..**

Eq. 1.2-1

$$SOP = \underbrace{\begin{pmatrix} \cos \theta & -\sin \theta \\ \sin \theta & \cos \theta \end{pmatrix}}_{-\theta} \underbrace{\frac{1}{\sqrt{2}} \begin{pmatrix} 1 & 1 \\ -1 & 1 \end{pmatrix}}_{+\pi/4} \underbrace{\begin{pmatrix} e^{-j\phi/2} & 0 \\ 0 & e^{+j\phi/2} \end{pmatrix} \frac{1}{\sqrt{2}} \begin{pmatrix} 1 \\ 1 \end{pmatrix}}_{\frac{1}{\sqrt{2}} \begin{pmatrix} e^{-j\phi/2} \\ e^{+j\phi/2} \end{pmatrix}} = \begin{pmatrix} \cos \frac{\phi}{2} \cos \theta - j \sin \frac{\phi}{2} \sin \theta \\ \cos \frac{\phi}{2} \sin \theta + j \sin \frac{\phi}{2} \cos \theta \end{pmatrix}$$

$$\frac{1}{2} \begin{pmatrix} e^{-j\phi/2} + e^{+j\phi/2} \\ -e^{-j\phi/2} + e^{+j\phi/2} \end{pmatrix} = \begin{pmatrix} \cos \frac{\phi}{2} \\ j \sin \frac{\phi}{2} \end{pmatrix}$$

And  $\varphi, \theta$  are the parameters that indicate the polarization state of the signal. The equivalent graphical representation for these parameters can be seen in the figure below:

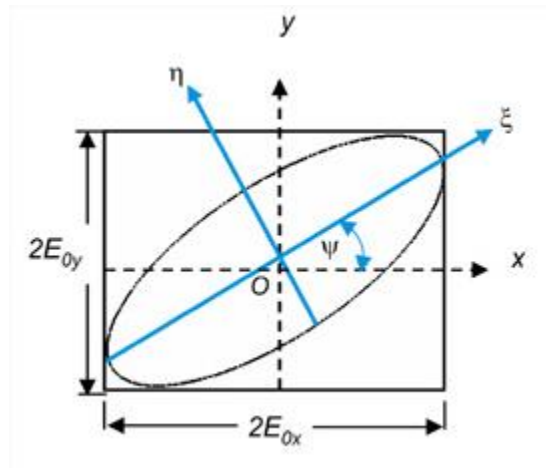


Figure 1.2-1. Signal polarization representation [1]



# Chapter 2 Devices

## 2.1. Optical fiber

### 2.1.1. Atenuation in optical fibers

When light propagates through the fiber, it experiences an exponential decay of the optical power over the distance as a consequence of absorption and scattering phenomena.

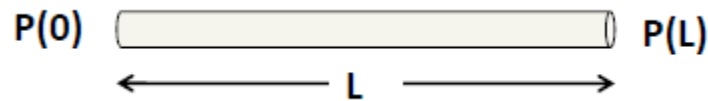


Figure 2.1-1. Optical fiber

Eq. 2.1-1

$$\frac{P(L)}{P(0)} = A = 10^{-\alpha L/10}$$

$$\alpha = \frac{1}{L} \log \left( \frac{P(0)}{P(L)} \right) \quad [dB/Km]$$

Any material absorbs energy at certain wavelengths corresponding to the electronic and vibrational resonances of the medium. There are two kinds of absorption: the intrinsic, which is due to the basic material (SiO<sub>2</sub>), and the extrinsic absorption, which is due to the impurities in the material.

There are two main scattering sources on optical fibers: the Rayleigh and the Mie scattering. The Rayleigh scattering, which is the most important, is the fundamental loss mechanism arising from microscopic density fluctuations which induce small variations of the refractive index of the material. The Mie scattering is a loss mechanism arising from cylindrical structure imperfections, comparable to the wavelength of the waveguide.

In the figure below, the main attenuation causes described before are represented depending on the wavelength.

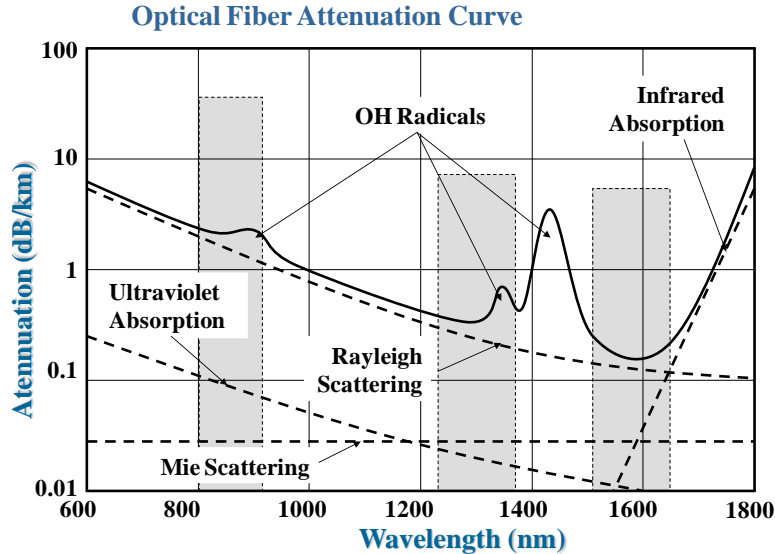


Figure 2.1-2. Optical fiber attenuation

## 2.1.2. Dispersion in optical fibers

The dispersion in optical fibers can be classified as follows:

- Intermodal dispersion
- Intramodal dispersion
  - Group Velocity Dispersion (GVD)
    - Waveguide Dispersion
    - Material Dispersion
  - Polarization mode dispersion(PMD)

The intermodal dispersion leads to an important broadening of optical pulses. From the geometrical-optics point of view, such broadening is attributed to different rays following different paths. In the modal description it is attributed to different modes having different group velocities.

The main advantage of single-mode fibers is the absence of intermodal dispersion because the energy of the pulse injected is transported just by one mode. Nevertheless, the dispersion does not disappear at all. That's because the group velocity associated with the fundamental mode is frequency dependent due to the chromatic dispersion. As a result, it is produced a phenomena called *group velocity dispersion* (GVD), which has two contributions: waveguide dispersion and material dispersion [2].

Within the intramodal dispersion, it also has to be considered the PMD. The latter is caused because the refractive index is polarization dependent, and so each component has a different GV.

In a single-mode fiber of length  $L$ , a specific spectral component would arrive at the end of the fiber with a delay  $T=L/v_g$ , where  $v_g$  –group velocity- is defined by:

**Eq. 2.1-2**

$$v_g = (d\beta/d\omega)^{-1}$$

Using  $\beta = n\omega/c$ , where  $n$  is the effective refractive index, then  $v_g = c/n_g$  where  $n_g$ , called mode index, is defined as:

**Eq. 2.1-3**

$$n_g = n + \omega(dn/d\omega)$$

If  $\Delta\omega$  is the spectral width pulse, the pulse broadening is expressed by:

**Eq. 2.1-4**

$$\Delta T = \frac{\delta T}{\delta\omega} \Delta\omega = \frac{\delta(\tau_g L)}{\delta\omega} \Delta\omega = L \frac{\delta^2\beta}{\delta\omega^2} \Delta\omega = L\beta_2 \Delta\omega$$

The parameter  $\beta_2$ , typically expressed in ps/GHz/Km, is known as the GVD parameter, which determines how much an optical pulse will broaden on propagation inside the fiber. Alternatively,

**Eq. 2.1-5**

$$\Delta T = \frac{\delta}{\delta\lambda} \left( \frac{L}{v_g} \right) \Delta\lambda = DL\Delta\lambda$$

where

**Eq. 2.1-6**

$$D = \frac{\delta}{\delta\lambda} \left( \frac{1}{v_g} \right) = \frac{2\pi c}{\lambda^2} \beta_2$$

$D$  is called the dispersion parameter and is typically expressed in ps/Km/nm

In order to study properly the dispersion in singlemode optical fibers, it is necessary to make an approach to the fiber transfer function in linear regime, which can be expressed as follows:

**Eq. 2.1-7**

$$H(\omega) = e^{-j\beta(\omega)L}$$

Where the propagation constant -  $\beta$ - is frequency dependent. As we want to have a simple expression for the transfer function, we can use the first terms of the Taylor series of  $\beta$  close to the carrier frequency ( $\omega_c$ ):

$$\beta(\omega) \approx \beta_0 + \beta_1(\omega - \omega_c) + \frac{1}{2}\beta_2(\omega - \omega_c)^2 + \frac{1}{6}\beta_3(\omega - \omega_c)^3$$

where  $\beta_n \equiv \frac{\partial \beta^n}{\partial \omega^n}$

From the former equation, the zero order term is a phase constant, the first order term is a delay, the second order term is the chromatic dispersion, and the third order term is the chromatic dispersion slope. As usual, we will omit the first two terms without loss of generality. We will neglect the last term for simplicity.

Therefore, the only term left is the second order term, which is precisely the dispersion parameter,  $\beta_2$ :

**Eq. 2.1-8**

$$H(\omega) = e^{-j\frac{1}{2}\beta_2(\omega-\omega_c)^2}$$

**2.1.3. Mathematical model**

In this case, as we always consider the singlemode fiber, the intermodal dispersion does not exist. Therefore, the fiber model implemented only considers the intramodal dispersion, more specifically the material and waveguide dispersion, which together are also called GVD plus the attenuation.

**Eq. 2.1-9**

$$E_{out}(t) = FFT^{-1}((e^{-\left(\frac{j\pi D \lambda^2 L f^2}{c}\right)}/A) \cdot FFT(E_{in}(t)))$$

where  $D(\text{ps/Km/nm})$  is the dispersion parameter about which we talked about in point 2.1.2,  $\lambda$  is the signal wavelength and  $A$  is the attenuation parameter defined in Eq. 2.1-1.

## 2.2. Photodetector PIN

### 2.2.1. Working principle

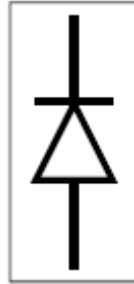


Figure 2.2-1. Photodetector PIN

The working principle of the photodetector PIN is the stimulated absorption, which is a quantum mechanics process that consists in stimulating electrons from incident photons.

Basically, the incident photon is absorbed by an electron, which increments its energy level. As a result of this, the greater number of photons received by the device, the greater amount of electrons will increment its energy level and pass from the ground state to excited state.

This process is explained in the following image:

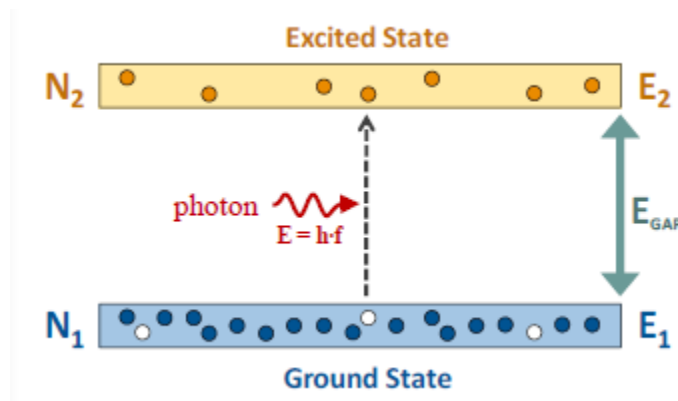


Figure 2.2-2. Stimulated absorption

In order to produce this effect, the photon's energy has to be greater than the energy gap between the ground state and the excited state. Therefore, the equation 2.4.1 has to be accomplished:

Eq. 2.2-1

$$hf \geq E_g \rightarrow \lambda \leq \frac{h \cdot c}{E_g} \equiv \lambda_c$$

As it is shown in the previous equation, the photon to electron conversion depends on the photon's frequency, so the intensity of the detected signal will be frequency dependent too,

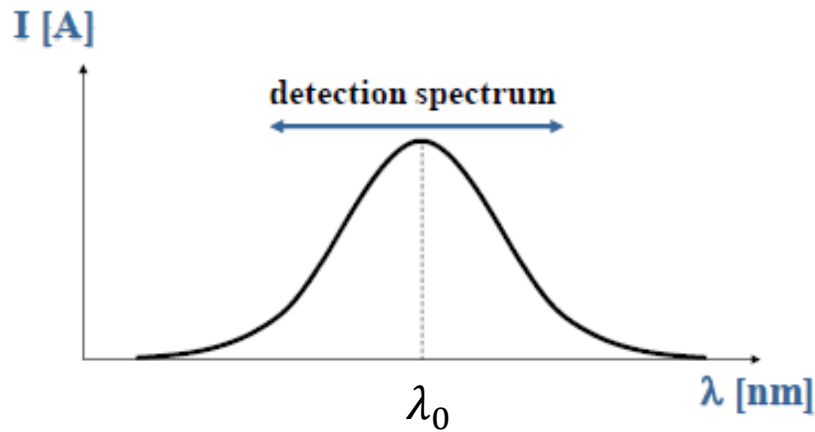


Figure 2.2-3. Photodetector detection spectrum

### 2.2.2. Parameters

There are two important parameters that measure the right behaviour of the photodetector: the **quantum efficiency** and the **responsivity**. The quantum efficiency, which depends basically on the materials used and structure of the device, is the measure of the photon-electron conversion efficiency, and can be expressed as shown in the Eq. 2.2-2

Eq. 2.2-2

$$\eta = \frac{\langle N^{\circ}e - h/seg \rangle}{\langle N^{\circ}fot/seg \rangle} = \frac{I_p/q}{P_{IN}/hf} \leq 1$$

The responsivity is the average delivered photocurrent over average incident optical power ratio, in other words, the transfer function of the photodetector.

Eq. 2.2-3

$$R = \frac{I_p}{P_{IN}} = \eta \frac{q}{hf} = \eta \frac{q \lambda}{h c} \quad [A/W]$$

### 2.2.3. Mathematical model

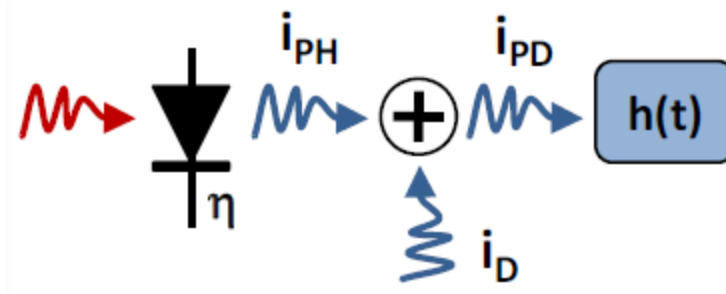


Figure 2.2-4. PIN photodetector model

Until now, we have been talking about the general concepts about the behavior of this device. If the device was perfect, then it would be just enough with the Eq. 2.2-3 to generate a good mathematical model for the PIN photodetector. However, we have to take into account an additional parameter, the dark current.

The **dark current [1]** is defined as the current through the photodiode in the absence of light. It includes photocurrent generated by background radiation and the saturation current of the semiconductor junction. In fact, we consider that the total electrical intensity delivered by the device is the sum of the ideal photocurrent - Eq. 2.2-3- and the dark current [3].

#### Eq. 2.2-4

$$i_{PD} = i_{PH} + i_D$$

#### Eq. 2.2-5

$$I_{PH} = \langle i_{PH} \rangle \geq R \cdot P_{IN}$$

$$\sigma_{PH}^2 = 2qB \cdot I_{PH}$$

Photodiodes have two different sources of noise: shot and thermal noise. The shot current refers to random fluctuations in the photocurrent due to light's inner randomness.

#### Eq. 2.2-6

$$i_{PH} = \langle i_{PH} \rangle + (i_{PH} - \langle i_{PH} \rangle)$$

If we define the shot noise as  $s = i_{PH} - \langle i_{PH} \rangle$ , the mean value and variance of  $s$  are:

#### Eq. 2.2-7

$$\langle s \rangle = 0$$

$$\sigma_s^2 = E\{s^2\} = E\{(i_{PH} - \langle i_{PH} \rangle)^2\}$$

Finally, if we make a slow signal approximation, the expression for shot noise variance is [2]:

**Eq. 2.2-8**

$$\sigma_{PH}^2(t) = 2qBRP(t)$$

The thermal noise, though, is very common in all kind of communication systems, and is usually the most important contribution of noise to an optical signal. It refers to the random fluctuations of the signal due to the chaotic movement of electrons in any electronic device or circuit.

**Eq. 2.2-9**

$$\langle i_{TH} \rangle = 0$$

$$\sigma_{TH}^2 = \langle i_{TH}^2 \rangle = 4 \frac{KT}{R_L} B$$



## 2.3.X coupler

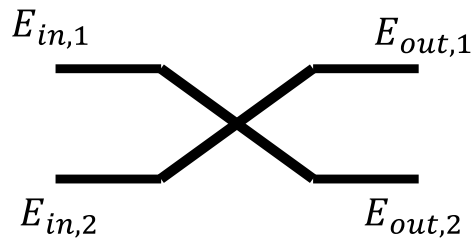


Figure 2.3-1. 3dB coupler model

The 3dB coupler is an optical device that can be used as a power splitter or a power combiner. As shown in Figure 2.3-1. 3dB coupler model, it has two inputs and two outputs.

So if the two inputs and just one output are used, the device will behave as an optical coupler where any of the output branches can be chosen. If one input and two outputs are used, then the device will behave as a signal splitter.

The coupler transfer function can be expressed as:

Eq. 2.3-1

$$\begin{pmatrix} E_{out,1} \\ E_{out,2} \end{pmatrix} = \begin{pmatrix} \sqrt{1-\alpha} & j\sqrt{\alpha} \\ j\sqrt{\alpha} & \sqrt{1-\alpha} \end{pmatrix} \begin{pmatrix} E_{in,1} \\ E_{in,2} \end{pmatrix}$$

where  $\alpha$  is the splitting factor.

## 2.4. Interferometer

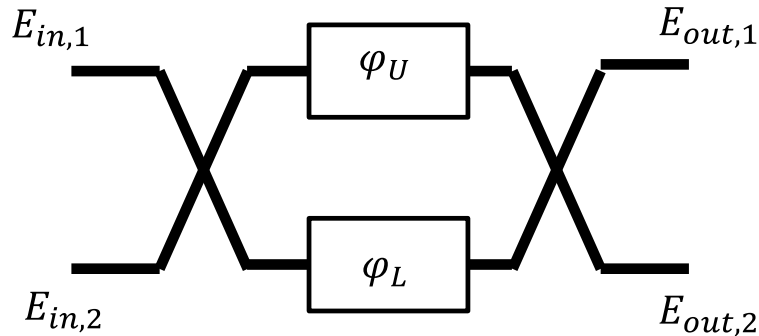


Figure 2.4-1. Interferometer model

The interferometer is a device which is used in receiver systems of multilevel modulations. Is the key device of the I/Q demodulator, which is the base for advanced modulation formats. It can be splitted in four simpler components: 2 couplers (see **¡Error! No se encuentra el origen de la referencia.¡Error! No se encuentra el origen de la referencia.** for more information) and 2 phase shifters. Therefore, the mathematical expression of the output is:

Eq. 2.4-1

$$\begin{aligned} \begin{pmatrix} E_{out,1} \\ E_{out,2} \end{pmatrix} &= \underbrace{\frac{1}{\sqrt{2}} \begin{pmatrix} 1 & j \\ j & 1 \end{pmatrix}}_{\text{coupler}} \underbrace{\begin{pmatrix} e^{j\phi_U} & 0 \\ 0 & e^{j\phi_L} \end{pmatrix}}_{\text{delay}} \underbrace{\frac{1}{\sqrt{2}} \begin{pmatrix} 1 & j \\ j & 1 \end{pmatrix}}_{\text{coupler}} \begin{pmatrix} E_{in,1} \\ E_{in,2} \end{pmatrix} = \\ &= \frac{1}{2} \begin{pmatrix} e^{j\phi_U} - e^{j\phi_L} & j(e^{j\phi_U} + e^{j\phi_L}) \\ j(e^{j\phi_U} + e^{j\phi_L}) & e^{j\phi_L} - e^{j\phi_U} \end{pmatrix} \begin{pmatrix} E_{in,1} \\ E_{in,2} \end{pmatrix} \end{aligned}$$

## 2.5. Mach Zender Modulator (MZM)

### 2.5.1. Working principle

A MZM is a device which can be used for controlling the power and phase of a laser beam through an electrical control signal. It typically contains one or more Pockels cells, whose principle of operation is based on the linear electro-optic effect -also called Pockels effect- which consists on the modification of the refractive index of a nonlinear crystal by an electric field in proportion to the field strength [4]. In the figure below is shown how the refractive index and the phase shift change by the applied voltage.

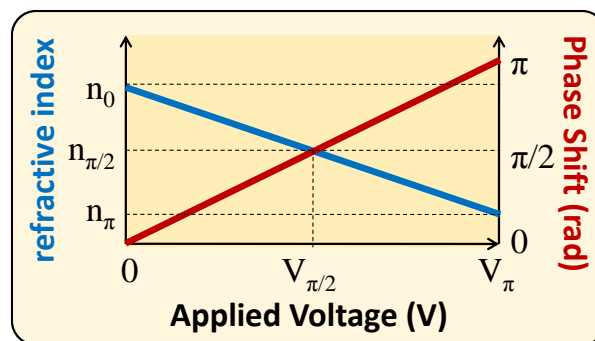


Figure 2.5-1. Pockels effect and phase shift in MZM [3]

There are two possible waveguide configurations for MZM to control the phase of the signal. If the waveguide has two electrodes on each side of the Pockels cells (as shown in figure XXX) and the electrical signal is applied, then the optical signal needs to be X polarized in order to be parallel to the electrical field. If the waveguide has the active electrode on top of the Pockels cell plus two ground electrodes on each side (as shown in figure XXX), then the optical signal needs to be Y polarized in order to be parallel to the electrical field.

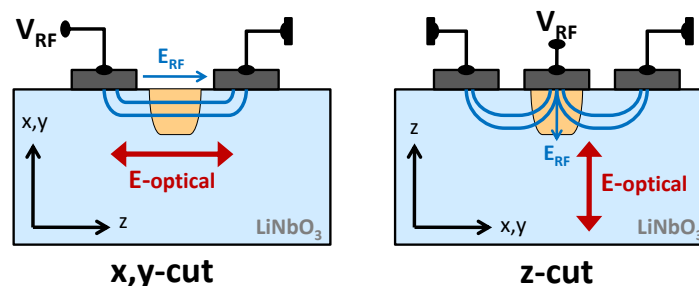


Figure 2.5-2. MZM polarization states

## 2.5.2. Mathematical model

### 2.5.2.1. MZM Transfer function

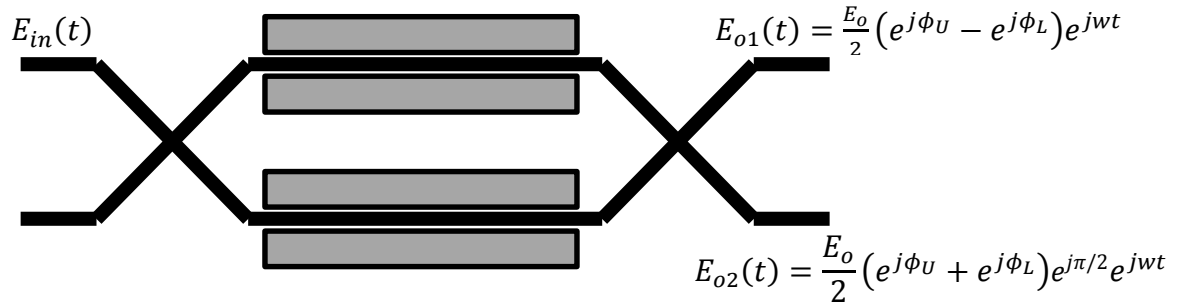


Figure 2.5-3. MZM model

The MZM is composed by two 3dB couplers and two electrical controlled phase shifters. So, the total transference function of this device can be expressed as:

#### Eq. 2.5-1

$$\begin{aligned} \begin{pmatrix} E_{out,1} \\ E_{out,2} \end{pmatrix} &= \underbrace{\frac{1}{\sqrt{2}} \begin{pmatrix} 1 & j \\ j & 1 \end{pmatrix}}_{\text{coupler}} \underbrace{\begin{pmatrix} e^{j\phi_U} & 0 \\ 0 & e^{j\phi_L} \end{pmatrix}}_{\text{delay}} \underbrace{\frac{1}{\sqrt{2}} \begin{pmatrix} 1 & j \\ j & 1 \end{pmatrix}}_{\text{coupler}} \begin{pmatrix} E_{in} \\ 0 \end{pmatrix} = \\ &= \frac{1}{2} \begin{pmatrix} e^{j\phi_U} - e^{j\phi_L} & j(e^{j\phi_U} + e^{j\phi_L}) \\ j(e^{j\phi_U} + e^{j\phi_L}) & e^{j\phi_L} - e^{j\phi_U} \end{pmatrix} \begin{pmatrix} E_{in} \\ 0 \end{pmatrix} = \frac{1}{2} \begin{pmatrix} e^{j\phi_U} - e^{j\phi_L} \\ j(e^{j\phi_U} + e^{j\phi_L}) \end{pmatrix} E_{in} \end{aligned}$$

Consider the structure of a MZM shown in the Figure 2.5-3. MZM model. If we define the input  $E_{in}(t)$  as:

#### Eq. 2.5-2

$$E_{in}(t) = E_0 e^{j\omega t}$$

A MZM is an interferometer with which a drive signal is used, producing a phase delay  $\phi_U$  and  $\phi_L$ , which are the upper and the lower branch delays respectively. Therefore, two possible outputs can be considered. In the case of this project, the lower branch has been chosen.

So, the output of our MZM model can be expressed as:

Eq. 2.5-3

$$E_{out}(t) = \frac{E_0}{2} (e^{j\phi_U} + e^{j\phi_L}) e^{\frac{j\pi}{2}} e^{j\omega t}$$

$$E_{out}(t) = \frac{E_0}{2} e^{j\frac{\phi_U + \phi_L}{2}} \underbrace{\left( e^{j\frac{\phi_U - \phi_L}{2}} + e^{-j\frac{\phi_U - \phi_L}{2}} \right)}_{2\cos\left(\frac{\phi_U - \phi_L}{2}\right)} e^{j\frac{\pi}{2}} e^{j\omega t} = E_0 \cos\left(\frac{\phi_U - \phi_L}{2}\right) e^{j\frac{\phi_U + \phi_L + \pi}{2}} e^{j\omega t}$$

Eq. 2.5-4

$$P_{out}(t) = P_0 \cos^2\left(\frac{\phi_U(t) - \phi_L(t)}{2}\right) = P_0 \cos^2\left(\pi \frac{V_U(t) - V_L(t)}{2V_\pi}\right)$$

$$\phi_{out}(t) = \frac{\phi_U(t) + \phi_L(t)}{2} = \pi \frac{V_U(t) + V_L(t)}{2V_\pi}$$

The Eq. 2.5-4 allows representing the MZM transfer function easily, and it is possible to see how the output power and phase evolve by the driving voltage. The module of the transfer function is represented on the figure below.

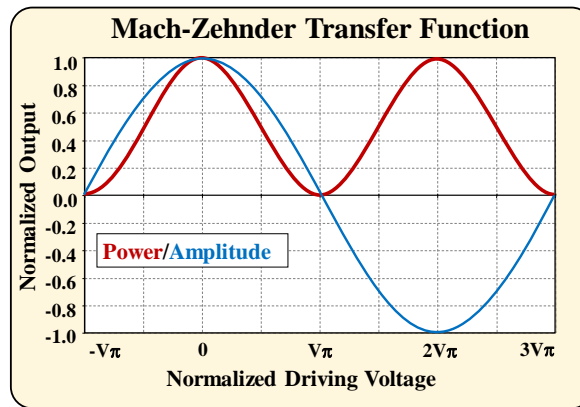


Figure 2.5-4. MZM transfer function

The delay on each branch of the MZM depends on several parameters, like the  $V_{\pi}$  voltage, which is the value for which there is an  $180^\circ$  phase shift at the output, the drive configuration-balanced and unbalanced- and the drive signal. Moreover, the MZM is polarization sensitive, and can be used in x-polarization or y-polarization mode. In conclusion, there are 4 possible configurations, which are discussed next.

### 2.5.2.2. Push-pull vs push-push operation

As shown in Eq. 2.5-3, the MZM output signal has frequency chirp, which means that its frequency present little variations on time. This effect can be problematic in some cases. For this reason the push-pull operation mode -explained below- is used.

When operating the MZM [5] in push-push mode – and identical phase shift  $\Phi = \Phi_U = \Phi_L$  is induced in both arms- a pure phase modulation is achieved. So, in this case the Eq. 2.5-3 becomes:

**Eq. 2.5-5**

$$E_{out}(t) = \frac{E_o}{2} (e^{j\phi_U} + e^{j\phi_L}) e^{\frac{j\pi}{2}} e^{j\omega t} = E_o e^{j\phi} e^{\frac{j\pi}{2}} e^{j\omega t} = E_{in}(t) e^{j\phi} e^{\frac{j\pi}{2}}$$

On the other hand [5], when one arm gets opposite phase shift with respect the other arm  $-\phi_U = -\phi_L$ , the MZM is operated in the push-pull mode and it is obtained a chirp free amplitude modulation, therefore the transfer function becomes:

**Eq. 2.5-6**

$$E_{out}(t) = \frac{E_o}{2} (e^{j\phi_U} + e^{j\phi_L}) e^{\frac{j\pi}{2}} e^{j\omega t} = E_{in}(t) \cos(\phi) e^{\frac{j\pi}{2}}$$

Where the output phase of the signal is cancelled:

**Eq. 2.5-7**

$$\phi_{out}(t) = \pi \frac{V_U(t) + V_L(t)}{2V_\pi} \xrightarrow{V_L(t) = -V_U(t)} 0$$

And the output power of the signal can be expressed as:

**Eq. 2.5-8**

$$P_{out}(t) = P_0 \cos^2 \left( \pi \frac{V_U(t) - V_L(t)}{2V_\pi} \right) \xrightarrow{V_L(t) = -V_U(t)} P_0 \cos^2 \left( \pi \frac{V_U(t)}{V_\pi} \right)$$

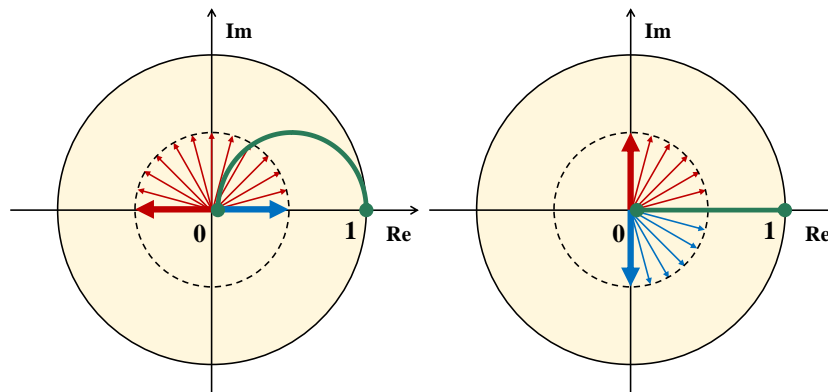


**Figure 2.5-5. Frequency chirp in MZM. Unbalanced operation(left),balanced operation(right)**

## 2.5.3. Drive configuration

### 2.5.3.1. xy-cut

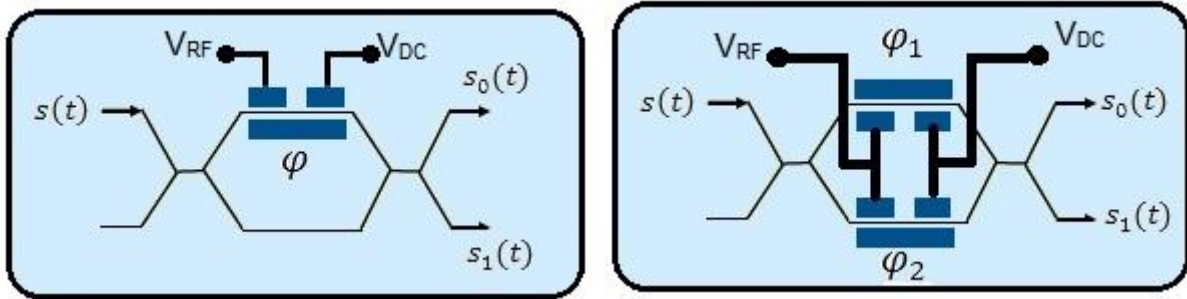


**Figure 2.5-6. MZM xy-cut and unbalanced (left) and balanced (right) drive model**

In the x-y cut configuration, the MZM is x-polarized. This means that the input signal has to be x-polarized too; otherwise there would be an important loss of signal power. The most commonly used is the balanced drive configuration, although it can also be used in an unbalanced drive mode.

The delay values of each branch depend on the drive configuration, so:

i) Unbalanced drive

**Eq. 2.5-9**

$$\phi_U = \frac{\pi}{V_\pi} (V_{RF} + V_{DC})$$

$$\phi_L = 0$$

ii) Balanced drive

**Eq. 2.5-10**

$$\phi_U = \frac{\pi}{V_\pi} (V_{RF} + V_{DC})$$

$$\phi_L = -\frac{\pi}{V_\pi} (V_{RF} + V_{DC})$$

## 2.5.3.2. z-cut

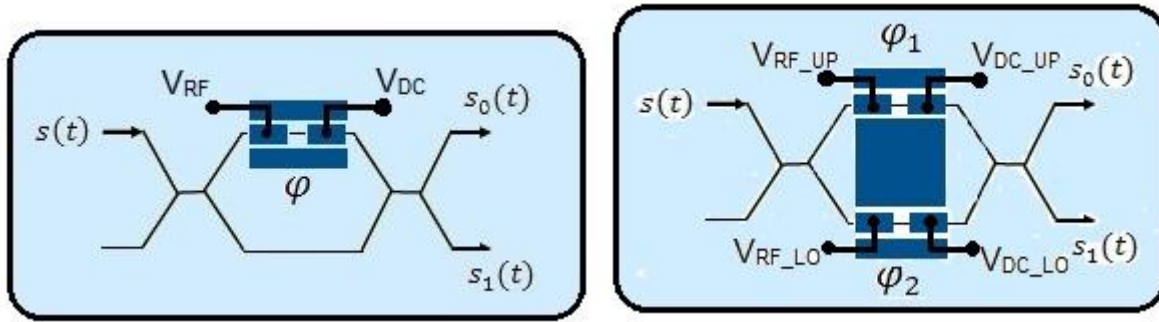


Figure 2.5-7. MZM z-cut and unbalanced (left) and balanced (right) drive

In this configuration, the MZM is y-polarized, so the input signal should be polarized the same way too. As shown in Figure 2.5-7. MZM z-cut and unbalanced (left) and balanced (right) drive, in the balanced configuration two drive signals are used. This allows having a better control of each branch delay. Nevertheless, if a symmetric configuration is needed, it is better to use an x-y configuration.

And the delay values:

i) Unbalanced drive

Eq. 2.5-11

$$\phi_U = \frac{\pi}{V_\pi} (V_{RF} + V_{DC})$$

$$\phi_L = 0$$

ii) Balanced drive

Eq. 2.5-12

$$\phi_U = \frac{\pi}{V_\pi} (V_{RF1} + V_{DC1})$$

$$\phi_L = \frac{\pi}{V_\pi} (V_{RF2} + V_{DC2})$$



### 2.5.4. Pulse carver

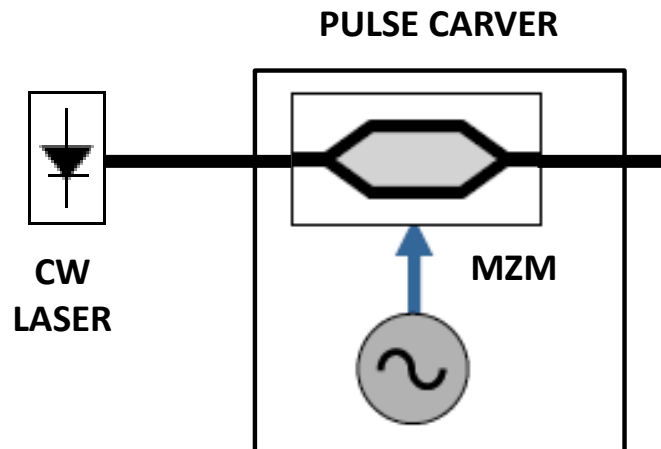


Figure 2.5-8. Pulse carver

MZM can also be used for another purpose in optical communications systems, the pulse carver. Pulse carver is a technique used to convert the optical pulses to an RZ format. It is useful for many reasons, for example it helps synchronizing the signal in the receiver.

It is possible to control the duty cycle of the output pulses by the local oscillator signal used as a drive signal for the MZM. There are three possible cases: 33%, 50% and 66% duty cycle, which are explained next.

#### 2.5.4.1. 33 % duty cycle

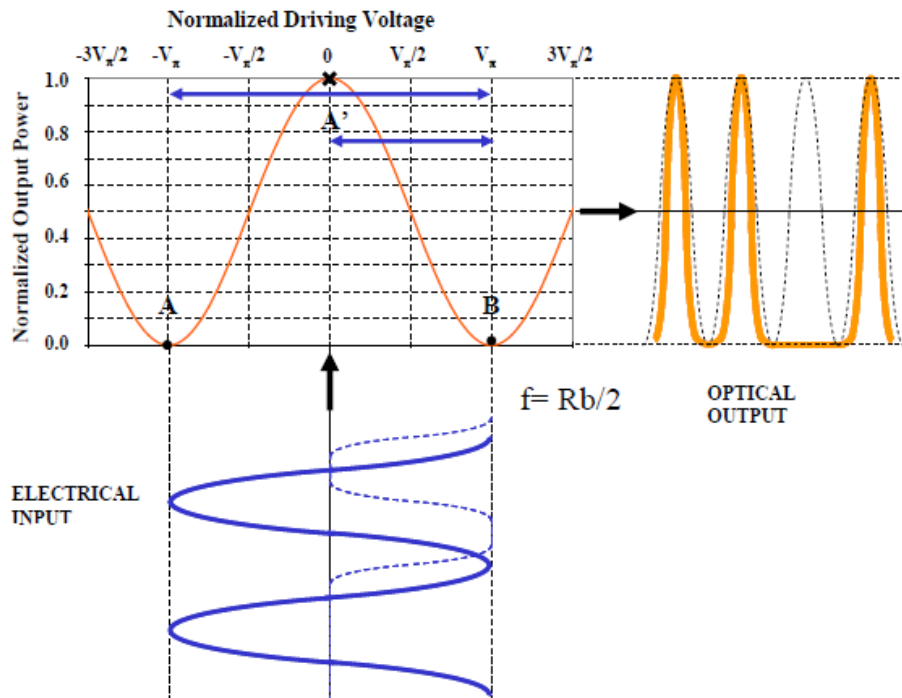


Figure 2.5-9. 33% duty cycle

In order to obtain a 33% duty cycle, the frequency of the electrical drive signal must be half the bitrate, and the amplitude must be between  $-V_{\pi}$  and  $V_{\pi}$ . Therefore the mathematical expression is:

Eq. 2.5-13

$$f_{OL}(t) = V_{\pi} \cos\left(2\pi \frac{R_{data}}{2} t\right)$$

2.5.4.2. 50% duty cycle

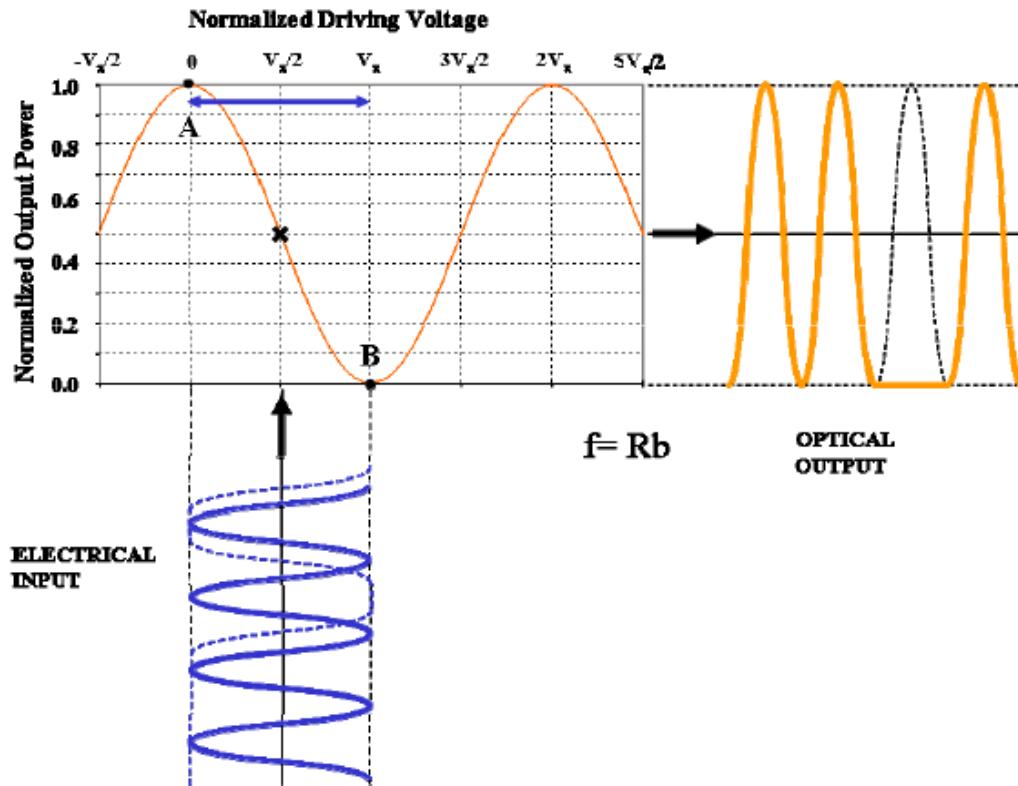


Figure 2.5-10. 50 % duty cycle

In the 50% case, it is needed a drive signal with amplitude between 0 and  $V_{\pi}$  and a frequency equal to the bitrate, hence the mathematical expression is:

$$f_{OL}(t) = V_{\pi} \frac{\cos(2\pi R_{data} t)}{2} + 0,5$$

### 2.5.4.3. 66% duty cycle

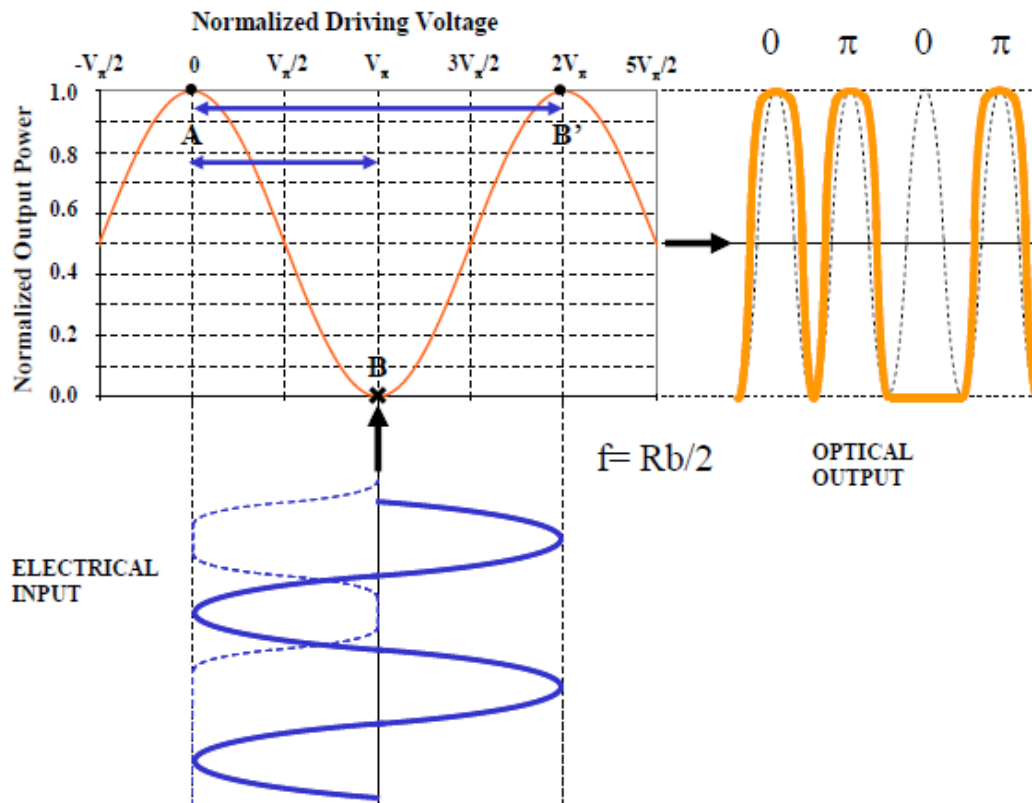


Figure 2.5-11. CSRZ pulse carver

This configuration is also called Carrier-suppressed mode, hence in this case are produced phase shifts of  $\pi$  to the output signal. This way of polarizing the Mach-Zender modulator is used to generate phase modulations.

The drive signal needed in order to achieve this is:

Eq. 2.5-14

$$f_{OL}(t) = V_{\pi} \left\{ \sin \left( 2\pi \frac{R_{data}}{2} t \right) + 1 \right\}$$

## 2.6. Optical Filters

Optical filters are used to selectively transmit or reject a wavelength or a range of wavelengths. There are many kinds of filters, but in communication systems the most important are the raised cosine filter and the Gaussian filter.

### 2.6.1. Raised cosine filter

Is the implementation of a band-pass Nyquist filter. Its description in the frequency domain is a piecewise function [6]

Eq. 2.6-1

$$H(f) = \begin{cases} T & |f| \leq \frac{1-\beta}{2T} \\ \frac{T}{2} \left[ 1 + \cos \left( \frac{\pi T}{\beta} \left[ |f| - \frac{1-\beta}{2T} \right] \right) \right] & \frac{1-\beta}{2T} < |f| \leq \frac{1+\beta}{2T} \\ 0 & \text{otherwise} \end{cases}$$

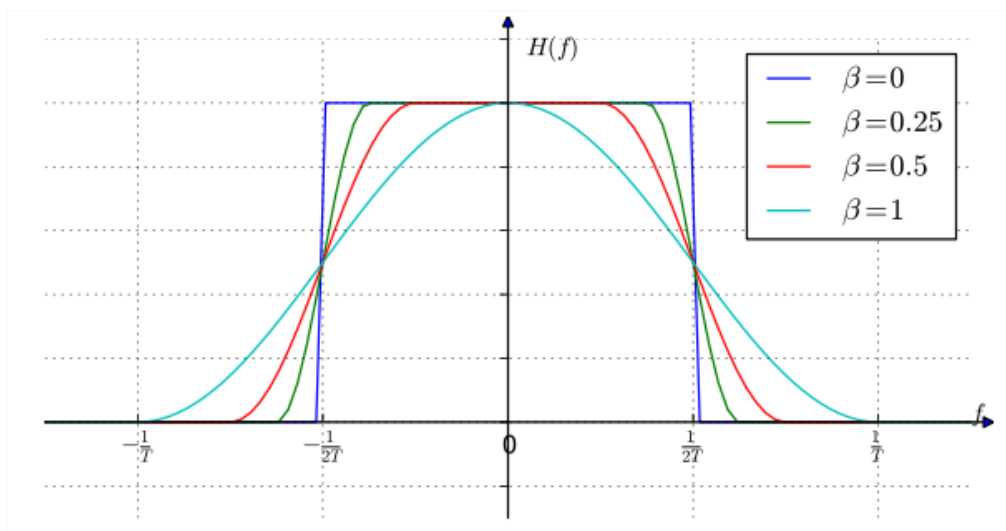


Figure 2.6-1. RCF Frequency domain impulse response [7]

In the previous figure it is represented the transfer function of the filter for different values of the roll-off factor ( $\beta$ ). For  $\beta=0$ , it is a perfect square filter, and as the roll-off factor is incremented, the flanks become softer.

In the time domain, though, the expression of the filter becomes a little bit simpler:

## Eq. 2.6-2

$$h(t) = \text{sinc}\left(\frac{t}{T}\right) \frac{\cos\left(\frac{\pi\beta t}{T}\right)}{1 - \frac{4\beta^2 t^2}{T^2}}$$

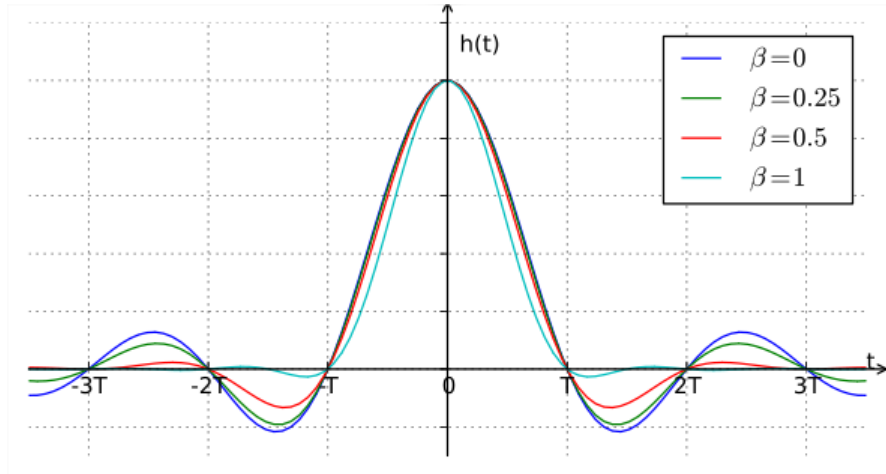


Figure 2.6-2. RCF time-domain transfer function [7]

## 2.6.2. Gaussian filter

The Gaussian filter has several practical applications. In the case of optical communication systems, it is commonly used to generate signals with smooth flanks, or even as band-pass filters needed in the TX/RX systems.

The transfer function can be expressed in the time-domain and frequency-domain, but as the Fourier transform of a Gaussian function is also a Gaussian function, the graphical representation is very similar, and is represented in Figure 2.6-3. Gaussian frequency transfer function

The only important parameters in the Gaussian filters are the mean value and the standard deviation (or variance). With the mean it is possible to control the central frequency of the filter, and the standard deviation indicates how wide the filter is, the higher the deviation the wider the filter becomes.

## Eq. 2.6-3

$$h(t) = \frac{1}{\sqrt{\pi} \cdot \sigma} e^{-\frac{t^2}{\sigma^2}} e^{j2\pi f_c t}$$

$$H(f) = e^{-(\pi(f-f_c)\sigma)^2}$$

Where  $\sigma$  is the standard deviation of the Gaussian function.

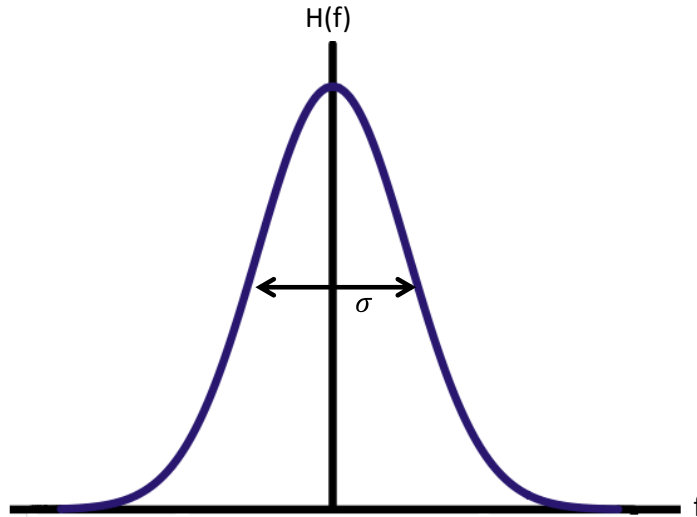


**Figure 2.6-3. Gaussian frequency transfer function**

It is very important to take into account the relationship between the optical signal bandwidth and the standard deviation of the filter. If we take the transfer function from Eq. 2.6-3 and seek the point where it is equal to  $1/\sqrt{2}$ , we will find the relationship we are looking for:

$$H(f - f_c = B_0) = e^{-(\pi B_0 \sigma)^2} = \frac{1}{\sqrt{2}}$$

$$-(\pi B_0 \sigma)^2 = -\frac{1}{2} \ln(2)$$

**Eq. 2.6-4**

$$B_0 = \frac{\sqrt{2 \ln(2)}}{2\pi\sigma}$$

# Chapter 3 Optical Modulations

## 3.1. Intensity Modulation

### 3.1.1. Transmitter OOK

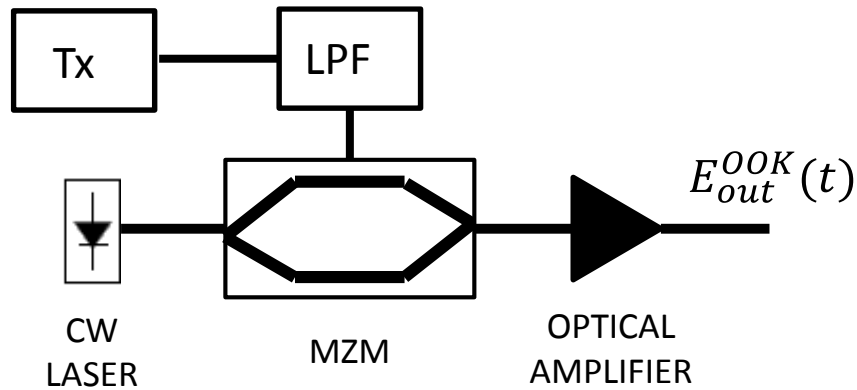


Figure 3.1-1. OOK transmitter

Eq. 3.1-1

$$\begin{pmatrix} E_{out,1}^{MZM} \\ E_{out,2}^{MZM} \end{pmatrix} = \frac{1}{2} \begin{pmatrix} e^{j\phi_U} - e^{j\phi_L} \\ j(e^{j\phi_U} + e^{j\phi_L}) \end{pmatrix} E_{in}(t)$$

As we saw in the chapter “Figure 2.5-4. MZM transfer function “, this device has two outputs, but the modulated signal is just one of them. So, in this case we have chosen the lower branch:

Eq. 3.1-2

$$\begin{aligned} E_{out}^{OOK} &= E_{out,1}^{MZM} = \frac{j}{2} (e^{j\phi_U} + e^{j\phi_L}) E_{in} \xrightarrow[\text{push-pull}]{\phi_L = -\phi_U} \\ &\xrightarrow[\text{push-pull}]{\phi_L = -\phi_U} \frac{j}{2} (e^{j\phi_U} + e^{-j\phi_U}) E_{in} = j \cos(\phi_U) E_{in} = \\ &= j \cos\left(\pi \frac{V_U(t)}{V_\pi}\right) E_{in} \end{aligned}$$

Where  $V_u(t)$  is the modulation signal from the upper branch, which must have an amplitude of  $V_{pi}/2$ .



### 3.1.2. Receiver OOK

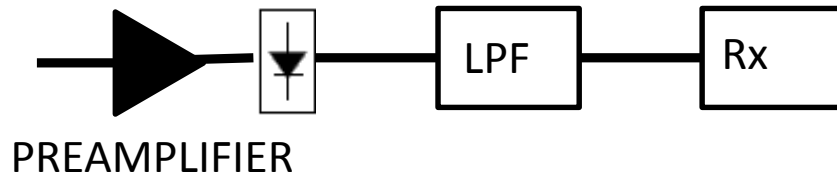


Figure 3.1-2. OOK receiver

The input signal received on the OOK receiver can be expressed as:

Eq. 3.1-3

$$E_{in}(t) = j \frac{E_0}{\sqrt{2}} \cos \phi_U(t) e^{j(\omega_c t + \theta)}$$

In the case of an OOK modulation, the receiver consists basically on a photodetector, so in order to obtain the expression for the demodulated signal we just need to calculate the signal module:

Eq. 3.1-4

$$I(t) = \Re |E_{in}(t)|^2 = \frac{E_0^2}{2} \cos^2 \left( \pi \frac{V_U(t)}{V_\pi} \right)$$

$$I(t = kT) = \frac{E_0^2}{2} \cos^2 \left( \pi \frac{V_U(t = kT)}{V_\pi} \right) = \xrightarrow{V_U(t = kT) = \left[ 0, \frac{V_\pi}{2} \right]} \left[ \frac{E_0^2}{2}, 0 \right]$$

## 3.3. Phase Modulation

### 3.3.1. Transmitter BPSK

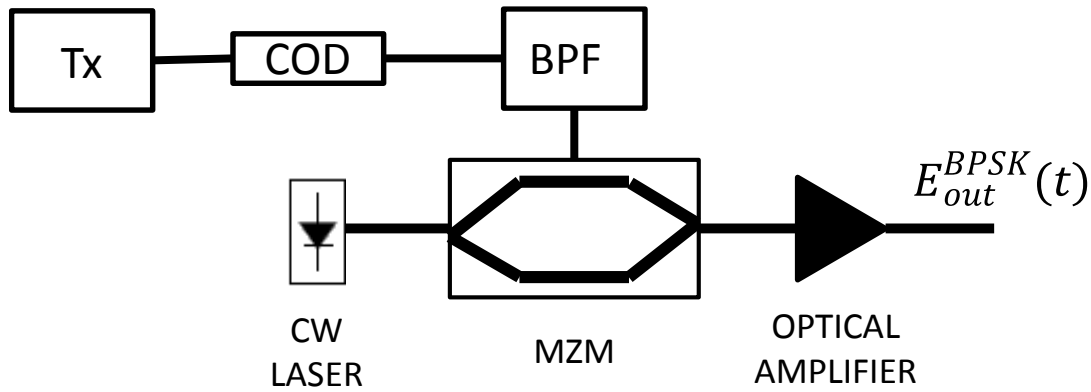


Figure 3.3-1. BPSK transmitter

Eq. 3.3-1

$$\begin{pmatrix} E_{out,1}^{MZM} \\ E_{out,2}^{MZM} \end{pmatrix} = \frac{1}{2} \begin{pmatrix} e^{j\phi_U} - e^{j\phi_L} \\ j(e^{j\phi_U} + e^{j\phi_L}) \end{pmatrix} E_{in}$$

As we saw in the chapter “Figure 2.5-4. MZM transfer function “, this device has two outputs, but the modulated signal is just one of them. So, in this case we have chosen the lower branch:

Eq. 3.3-2

$$\begin{aligned} E_{out}^{BPSK} &= E_{out,1}^{MZM} = \frac{j}{2} (e^{j\phi_U} + e^{j\phi_L}) E_{in} \xrightarrow[\text{push-pull}]{\phi_L = -\phi_U} \\ &\xrightarrow[\text{push-pull}]{\phi_L = -\phi_U} \frac{j}{2} (e^{j\phi_U} + e^{-j\phi_U}) E_{in} = j \cos(\phi_U) E_{in} = \\ &\quad \left( \pi \frac{V_U}{V_\pi} \right) \\ &= j \cos \left( \pi \frac{V_U(t)}{V_\pi} \right) E_{in} \end{aligned}$$

Therefore,

**Eq. 3.3-3**

$$E_{out}^{BPSK} \Big|_{t=kT_s} = j \frac{E_0}{2} \cos \left( \underbrace{\pi \frac{V_U(kT_s)}{V_\pi}}_{\phi_t} \right) = j \frac{E_0}{2} \cos(\phi_t), \phi_t = [0, \pi]$$

In the figure below it is shown the constellation for the BPSK modulation as it is used in our simulator:

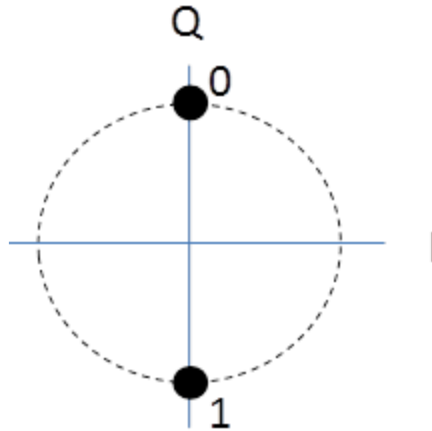


**Figure 3.3-2. BPSK constellation**

### 3.3.2. Receiver BPSK

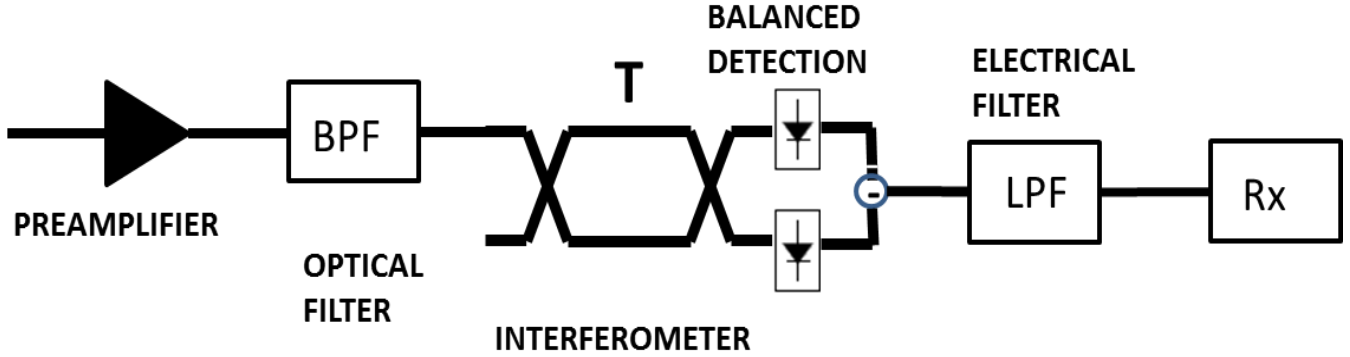


Figure 3.3-3. BPSK detector

If we define the input signal as shown in the following equation:

Eq. 3.3-4

$$E_{in}(t) = j \frac{E_0}{\sqrt{2}} \cos \phi_I(t) e^{j(\omega_c t + \theta)}$$

And then we use the interferometer transfer function, we obtain the two signals just before the photodetectors:

$$\begin{aligned} E_{out}^{MZI}(t) &= \frac{1}{2} \begin{pmatrix} \partial(t-T) - \partial(t) & j(\partial(t-T) + \partial(t)) \\ j(\partial(t-T) + \partial(t)) & \partial(t) - \partial(t-T) \end{pmatrix} * \begin{pmatrix} E_{in}(t) \\ 0 \end{pmatrix} = \\ &= \frac{1}{2} \begin{pmatrix} E_{in}(t-T) - E_{in}(t) \\ j\{E_{in}(t-T) + E_{in}(t)\} \end{pmatrix} = \\ &= \frac{E_0}{2\sqrt{2}} \begin{pmatrix} \cos \phi_I(t-T) e^{j(\omega_c(t-T) + \theta)} - \cos \phi_I(t) e^{j(\omega_c t + \theta)} \\ j\{\cos \phi_I(t-T) e^{j(\omega_c(t-T) + \theta)} + \cos \phi_I(t) e^{j(\omega_c t + \theta)}\} \end{pmatrix} \xrightarrow{\omega_c T = 2n\pi} = \\ &= \frac{E_0}{2\sqrt{2}} \begin{pmatrix} \cos \phi_I(t-T) - \cos \phi_I(t) \\ j\{\cos \phi_I(t-T) + \cos \phi_I(t)\} \end{pmatrix} e^{j(\omega_c t + \theta)} \end{aligned}$$

Finally, the signal passes through the photodetectors and we get the expressions below:

$$\begin{aligned} I(t) &= \Re \left\{ |E_{out,1}^{MZI}(t)|^2 - |E_{out,2}^{MZI}(t)|^2 \right\} \\ |E_{out,1}^{MZI}(t)|^2 &= \frac{E_0^2}{8} \{ \cos^2 \phi_I(t-T) + \cos^2 \phi_I(t) - 2 \cos \phi_I(t-T) \cos \phi_I(t) \} \\ |E_{out,2}^{MZI}(t)|^2 &= \frac{E_0^2}{8} \{ \cos^2 \phi_I(t-T) + \cos^2 \phi_I(t) + 2 \cos \phi_I(t-T) \cos \phi_I(t) \} \end{aligned}$$

$$I(t) = -\frac{\Re E_0^2}{2} \cos \phi_i(t-T) \cos \phi_i(t)$$

And if we discretize the signal in time, the expression for the DBPSK precoder is finally obtained:

$$I(t = kT) = -\frac{\Re E_0^2}{2} \cos \phi_{k-1} \cos \phi_k = -\Re E_0^2 \cos \Delta \phi_k$$

And the truth table is the following:

$I_k$	$I_{k-1}$	$\Phi_k$	$\Phi_{k-1}$	$\nabla \Phi$	$u_k$
0	0	0	0	0	0
0	1	0	$\pi$	$\pi$	0
1	0	$\pi$	0	$\pi$	1
1	1	$\pi$	$\pi$	0	1

Table 3.3-1. Truth table for BPSK

Eq. 3.3-5

$$I_k = u_k \otimes I_{k-1}$$

So, the expression of the pre-coder function for DBPSK modulation is shown in Eq. 3.3-4.

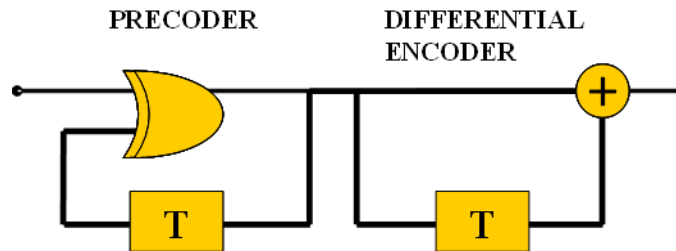


Figure 3.3-4. Implementation of the DBPSK precoder

### 3.3.3. Transmitter QPSK

So as to obtain the pre-coder logical expression, we need to take a closer look to the DQPSK transmitter and receiver systems. In the figure below, it is shown the architecture of a DQPSK transmitter.

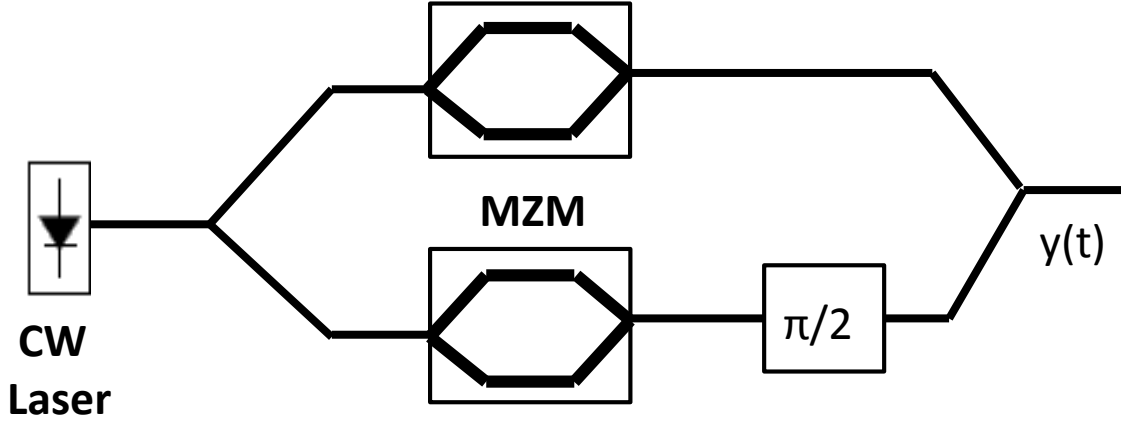


Figure 3.3-5: I/Q modulator

As seen in section 2.5.2, the output of a MZM can be expressed as:

Eq. 3.3-1

$$E_{out,2}^{MZM} = \frac{j}{2} (e^{j\phi_U} + e^{j\phi_L}) E_{in}^{MZM}$$

Therefore, in order to obtain the output of the I/Q modulator, we just have to multiply the transfer functions of all the elements that compose it:

$$\begin{aligned} \begin{pmatrix} E_{out,1}^{IQM} \\ E_{out,2}^{IQM} \end{pmatrix} &= \underbrace{\frac{1}{\sqrt{2}} \begin{pmatrix} 1 & j \\ j & 1 \end{pmatrix}}_{coupler} \underbrace{\begin{pmatrix} 1 & 0 \\ 0 & j \end{pmatrix}}_{phase\_shift} \underbrace{\frac{j}{2} \begin{pmatrix} e^{j\phi_U^I} + e^{j\phi_L^I} & 0 \\ 0 & e^{j\phi_U^O} + e^{j\phi_L^O} \end{pmatrix}}_{MZMs} \underbrace{\frac{1}{\sqrt{2}} \begin{pmatrix} 1 & j \\ j & 1 \end{pmatrix}}_{coupler} \begin{pmatrix} E_{in} \\ 0 \end{pmatrix} = \\ &= \frac{j}{4} \begin{pmatrix} 1 & j \\ j & 1 \end{pmatrix} \begin{pmatrix} e^{j\phi_U^I} + e^{j\phi_L^I} & 0 \\ 0 & j(e^{j\phi_U^O} + e^{j\phi_L^O}) \end{pmatrix} \begin{pmatrix} 1 & j \\ j & 1 \end{pmatrix} \begin{pmatrix} E_{in} \\ 0 \end{pmatrix} = \\ &= \frac{j}{4} \begin{pmatrix} 1 & j \\ j & 1 \end{pmatrix} \begin{pmatrix} e^{j\phi_U^I} + e^{j\phi_L^I} & j(e^{j\phi_U^I} + e^{j\phi_L^I}) \\ -(e^{j\phi_U^O} + e^{j\phi_L^O}) & j(e^{j\phi_U^O} + e^{j\phi_L^O}) \end{pmatrix} \begin{pmatrix} E_{in} \\ 0 \end{pmatrix} = \\ &= \frac{1}{4} \begin{pmatrix} j(e^{j\phi_U^I} + e^{j\phi_L^I}) + (e^{j\phi_U^O} + e^{j\phi_L^O}) \\ -(e^{j\phi_U^I} + e^{j\phi_L^I}) - j(e^{j\phi_U^O} + e^{j\phi_L^O}) \end{pmatrix} E_{in} \end{aligned}$$

So the transfer function of the I/Q modulator is:

**Eq. 3.3-2**

$$\begin{pmatrix} E_{out,1}^{IQM} \\ E_{out,2}^{IQM} \end{pmatrix} = \frac{1}{4} \begin{pmatrix} j(e^{j\phi_U^I} + e^{j\phi_L^I}) + (e^{j\phi_U^Q} + e^{j\phi_L^Q}) \\ -(e^{j\phi_U^I} + e^{j\phi_L^I}) - j(e^{j\phi_U^Q} + e^{j\phi_L^Q}) \end{pmatrix} E_{in}$$

But as we already did with the MZM, we are only interested in one of the outputs, which will be our modulated signal. In this case, the second output branch is chosen:

$$\begin{aligned} E_{out,2}^{IQM} &= -\frac{1}{4} \left\{ (e^{j\phi_U^I} + e^{j\phi_L^I}) + j(e^{j\phi_U^Q} + e^{j\phi_L^Q}) \right\} E_{in} = \\ &= -\frac{1}{2} \left\{ \underbrace{\cos\left(\frac{\phi_U^I - \phi_L^I}{2}\right)}_{\left(\frac{V_U^I - V_L^I}{\pi 2V_\pi}\right)} e^{j\frac{\phi_U^I + \phi_L^I}{2}} + j \underbrace{\cos\left(\frac{\phi_U^Q - \phi_L^Q}{2}\right)}_{\left(\frac{V_U^Q - V_L^Q}{\pi 2V_\pi}\right)} e^{j\frac{\phi_U^Q + \phi_L^Q}{2}} \right\} E_{in} \xrightarrow[\text{push-pull}]{\substack{\phi_L^I = -\phi_U^I \\ \phi_L^Q = -\phi_U^Q}} \\ &\xrightarrow[\text{push-pull}]{\substack{\phi_L^I = -\phi_U^I \\ \phi_L^Q = -\phi_U^Q}} -\frac{1}{2} \left\{ \underbrace{\cos(\phi_U^I)}_{\left(\frac{V_U^I}{\pi V_\pi}\right)} + j \underbrace{\cos(\phi_U^Q)}_{\left(\frac{V_U^Q}{\pi V_\pi}\right)} \right\} E_{in} = -\frac{1}{2} \left\{ \cos\left(\pi \frac{V_U^I(t)}{V_\pi}\right) + j \cos\left(\pi \frac{V_U^Q(t)}{V_\pi}\right) \right\} E_{in} \\ E_{out,1}^{IQM} \Big|_{t=kT_s} &= -\frac{E_0}{2} \left\{ \underbrace{\cos\left(\pi \frac{V_U^I(kT_s)}{V_\pi}\right)}_{\cos\phi_I} + j \underbrace{\cos\left(\pi \frac{V_U^Q(kT_s)}{V_\pi}\right)}_{\cos\phi_Q} \right\} = -\frac{E_0}{2} \{ \cos\phi_I + j \cos\phi_Q \} \end{aligned}$$

Finally,

**Eq. 3.3-3**

$$E_{out,1}^{QPSK} = -\frac{E_0}{2} \{ \cos\phi_I + j \cos\phi_Q \}, \phi_{I,Q} = [0, \pi]$$

In the figure below it can be seen the constellation of the DQPSK used in our simulator.

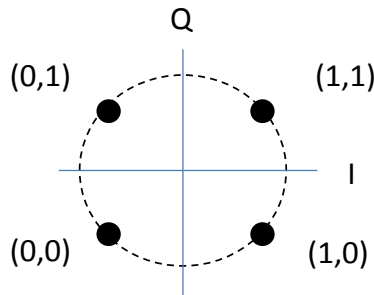


**Figure 3.3-6 . DQPSK constellation**

According to the information above, it is possible to find the phase of our signal depending on the I/Q values, which is detailed in the **¡Error! No se encuentra el origen de la referencia.**

I\Q	0	1
0	$-3\pi/4$	$3\pi/4$
1	$-\pi/4$	$\pi/4$

**Table 3.3-2. Signal Phase**



### 3.3.4. Receiver DQPSK

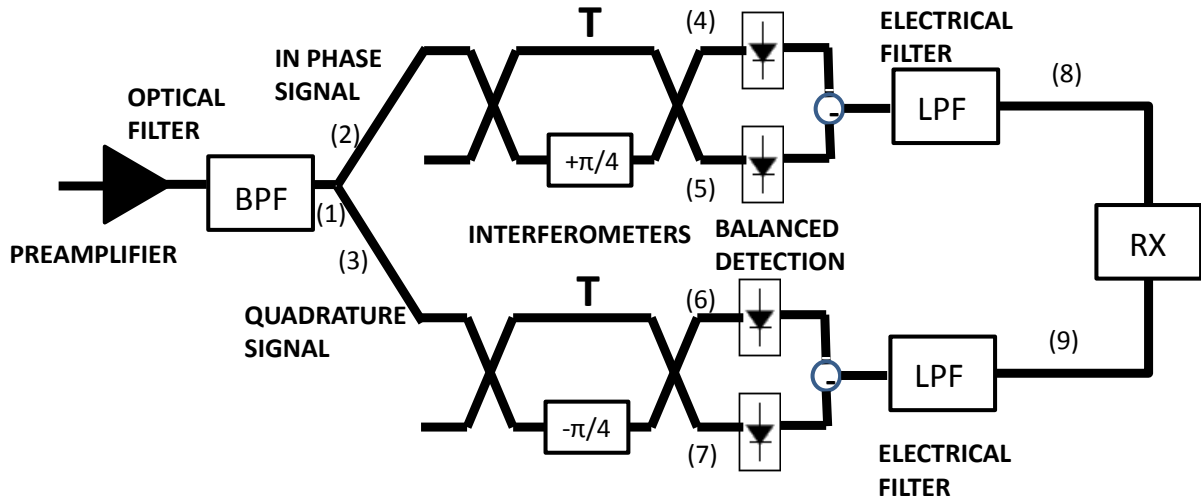


Figure 3.3-7. DQPSK Receiver architecture

In this point, as the incoming signal has been affected by propagation effects such as delay and attenuation, we don't know the phase and amplitude of the input signal. Therefore, we are going to define an arbitrary amplitude and phase:

Eq. 3.3-4

$$E_{in}(t) = \frac{E_0}{\sqrt{2}} \underbrace{\{\cos \phi_I(t) + j \cos \phi_Q(t)\}}_{\sqrt{2}M(t)e^{j\phi(t)}} e^{j(\omega_c t + \theta)} = E_0 M(t) e^{j\phi(t)} e^{j(\omega_c t + \theta)}$$

where

$$M(t) \equiv \sqrt{\frac{\cos^2 \phi_I(t) + \cos^2 \phi_Q(t)}{2}} \quad \phi(t) = \arctan \left\{ \frac{\cos \phi_Q(t)}{\cos \phi_I(t)} \right\}$$

If we take the expression for the XCoupler from 2.3, the input signals to each interferometer can be expressed as:

$$\begin{pmatrix} E_{out,1}^{XCo} \\ E_{out,2}^{XCo} \end{pmatrix} = \underbrace{\frac{1}{\sqrt{2}} \begin{pmatrix} 1 & j \\ j & 1 \end{pmatrix}}_{coupler} \begin{pmatrix} E_{in}(t) \\ 0 \end{pmatrix}$$

Eq. 3.3-5

$$E_{out-\begin{pmatrix} 1 \\ 2 \end{pmatrix}}^{XCo}(t) = \begin{pmatrix} 1 \\ j \end{pmatrix} \frac{E_0}{\sqrt{2}} M(t) e^{j\phi(t)} e^{j(\omega_c t + \theta)}$$

The next step is the interferometer. So, in this case we need the matrix found in 2.4. In order to make it simpler, we will use a compact notation to include for the two branches of the detector in the same expression. If we make the calculations:

$$\begin{aligned}
 E_{out}^{MZI-(l)}(t) &= \begin{pmatrix} 1 \\ j \end{pmatrix} \frac{1}{2} \begin{pmatrix} \partial(t-T) - \partial(t)e^{\pm j\phi_L} & j(\partial(t-T) + \partial(t)e^{\pm j\phi_L}) \\ j(\partial(t-T) + \partial(t)e^{\pm j\phi_L}) & \partial(t)e^{(\pm)j\phi_L} - \partial(t-T) \end{pmatrix} * \begin{pmatrix} E_{out-(1)}^{XC_o}(t) \\ 0 \end{pmatrix} = \\
 &= \begin{pmatrix} 1 \\ j \end{pmatrix} \frac{1}{2} \begin{pmatrix} E_{out-(1)}^{XC_o}(t-T) - E_{out-(1)}^{XC_o}(t)e^{\pm j\phi_L} \\ j \{ E_{out-(1)}^{XC_o}(t-T) + E_{out-(1)}^{XC_o}(t)e^{\pm j\phi_L} \} \end{pmatrix} = \\
 &= \begin{pmatrix} 1 \\ j \end{pmatrix} \frac{E_0}{2\sqrt{2}} \begin{pmatrix} M(t-T)e^{j\phi(t-T+\theta)}e^{j\omega_c(t-T)} - M(t)e^{j\phi(t)}e^{j(\omega_c t + \theta)}e^{\pm j\phi_L} \\ j \{ M(t-T)e^{j\phi(t-T+\theta)}e^{j\omega_c(t-T)} + M(t)e^{j\phi(t)}e^{j(\omega_c t + \theta)}e^{\pm j\phi_L} \} \end{pmatrix}
 \end{aligned}$$

### Eq. 3.3-6

Now assuming that there is an integer amount of period in a bit slot and particularizing the phase shift to 45° we get to the expression:

$$E_{out}^{MZI-(l)}(t) \Big|_{\substack{\omega_c T = 2n\pi \\ \phi_L = \pi/4}} = \begin{pmatrix} 1 \\ j \end{pmatrix} \frac{E_0}{2\sqrt{2}} \begin{pmatrix} M(t-T)e^{j\phi(t-T)} - M(t)e^{j\phi(t)}e^{\pm j\frac{\pi}{4}} \\ j \{ M(t-T)e^{j\phi(t-T)} + M(t)e^{j\phi(t)}e^{\pm j\frac{\pi}{4}} \} \end{pmatrix} e^{j(\omega_c t + \theta)}$$

The equation Eq. 3.3-6 shows the signal expression that we will have in the points (4)-(5) and (6)-(7) of the figure **¡Error! No se encuentra el origen de la referencia.**, respectively. Therefore, the last step is the photodetection:

### Eq. 3.3-7

$$I_{(l)}(t) = \Re \left\{ \left| E_{out,1}^{MZI-(l)}(t) \right|^2 - \left| E_{out,2}^{MZI-(l)}(t) \right|^2 \right\}$$

Where  $\Re$  is the responsivity of the photodetectors.

$$\begin{aligned}
 \left| E_{out,1}^{MZI-(I)}(t) \right|^2 &= \frac{E_0^2}{8} \left\{ M^2(t-T) + M^2(t) - 2M(t-T)M(t) \operatorname{Re} \left\{ e^{j\left\{ \phi(t-T) - \phi(t) \mp \frac{\pi}{4} \right\}} \right\} \right\} \\
 \left| E_{out,2}^{MZI-(I)}(t) \right|^2 &= \frac{E_0^2}{8} \left\{ M^2(t-T) + M^2(t) + 2M(t-T)M(t) \operatorname{Re} \left\{ e^{j\left\{ \phi(t-T) - \phi(t) \mp \frac{\pi}{4} \right\}} \right\} \right\} \\
 I_{(I)}^{(I)}(t) &= -\frac{\Re E_0^2}{2} M(t-T)M(t) \underbrace{\cos \left( \underbrace{\phi(t-T) - \phi(t)}_{\Delta\phi(t)} \mp \frac{\pi}{4} \right)}_{\cos\Delta\phi(t)\cos\frac{\pi}{4} \pm \sin\Delta\phi(t)\sin\frac{\pi}{4}} = \frac{\Re E_0^2}{2\sqrt{2}} M(t-T)M(t) \{ \cos\Delta\phi(t) \mp \sin\Delta\phi(t) \} \\
 I_{(I)}^{(I)}(t = kT) &= \frac{\Re E_0^2}{2\sqrt{2}} \underbrace{M([k-1]T)}_{\sqrt{2}} \underbrace{M(kT)}_{\sqrt{2}} \left\{ \underbrace{\cos\Delta\phi(kT)}_{\cos\Delta\phi_k} \mp \underbrace{\sin\Delta\phi(kT)}_{\sin\Delta\phi_k} \right\} = \frac{\Re E_0^2}{\sqrt{2}} \{ \cos\Delta\phi_k \mp \sin\Delta\phi_k \}
 \end{aligned}$$

Eq. 3.3-6

$$u = \mathbf{cos}(\nabla\varphi) - \mathbf{sin}(\nabla\varphi)$$

$$v = \mathbf{cos}(\nabla\varphi) + \mathbf{sin}(\nabla\varphi)$$

To find the pre-codification functions, the truth table is required:

$I_k$	$Q_k$	$I_{k-1}$	$Q_{k-1}$	$\Phi_k$	$\Phi_{k-1}$	$\nabla\Phi$	$u_k$	$v_k$
0	0	0	0	$-3\pi/4$	$-3\pi/4$	0	0	0
0	0	0	1	$-3\pi/4$	$3\pi/4$	$-\pi/2$	0	1
0	0	1	0	$-3\pi/4$	$-\pi/4$	$-3\pi/2$	1	0
0	0	1	1	$-3\pi/4$	$\pi/4$	$\pi$	1	1
0	1	0	0	$3\pi/4$	$-3\pi/4$	$\pi/2$	1	0
0	1	0	1	$3\pi/4$	$3\pi/4$	0	0	0
0	1	1	0	$3\pi/4$	$-\pi/4$	$\pi$	1	1
0	1	1	1	$3\pi/4$	$\pi/4$	$-\pi/2$	0	1
1	0	0	0	$-\pi/4$	$-3\pi/4$	$-3\pi/2$	0	1
1	0	0	1	$-\pi/4$	$3\pi/4$	$\pi$	1	1
1	0	1	0	$-\pi/4$	$-\pi/4$	0	0	0
1	0	1	1	$-\pi/4$	$\pi/4$	$\pi/2$	1	0
1	1	0	0	$\pi/4$	$-3\pi/4$	$\pi$	1	1
1	1	0	1	$\pi/4$	$3\pi/4$	$\pi/2$	1	0
1	1	1	0	$\pi/4$	$-\pi/4$	$-\pi/2$	0	1
1	1	1	1	$\pi/4$	$\pi/4$	0	0	0

Table 3.3-3. DQPSK precoder truth table

Now, to find the mathematical expressions of the I/Q functions, Karnaugh maps are needed:

		$I_{k-1} \quad Q_{k-1}$			
$u_k \quad v_k$		00	01	11	10
00				1	1
01	1				1
11	1	1			
10		1	1		

		$I_{k-1} \quad Q_{k-1}$			
$u_k \quad v_k$		00	01	11	10
00			1	1	
01				1	1
11	1				1
10	1	1			

**Table 3.3-4: Karnaugh maps for I (left) and Q (right) functions**

Therefore, the resulting functions are:

**Eq. 3.3-7**

$$I_k = \bar{Q}_{k-1}\bar{I}_{k-1}u_k + \bar{I}_{k-1}Q_{k-1}\bar{v}_k + Q_{k-1}I_{k-1}\bar{u}_k + I_{k-1}\bar{Q}_{k-1}v_k$$

$$Q_k = \bar{Q}_{k-1}\bar{I}_{k-1}v_k + \bar{I}_{k-1}Q_{k-1}u_k + Q_{k-1}I_{k-1}\bar{v}_k + I_{k-1}\bar{Q}_{k-1}\bar{u}_k$$

# Chapter 4 BER

## 4.1. Introduction

One of the most common requirements that have to meet an optical system is to have less than a specified Bit Error Rate(BER). BERs required are very low, usually 1 over  $10^{15}$ , and because of that it would take tens of years to obtain a BER estimation by the method of counting errors. Nevertheless, there are different ways to represent the signals, which allow us to obtain BER estimations with more ease than in a laboratory.

In systems with a single dominant type of degradation, analytical methods may be used to estimate BERs, as they are useful to obtain a first approximation. For instance, it can be used in systems without optical amplifiers, where the thermal noise is dominant or in systems with optical amplifiers where the Signal-ASE noise dominates.

An important parameter that needs to be used in optical simulation systems is the Q parameter. It is used to measure the optical signal quality, and it can be expressed as:

**Eq. 4.1-1**

$$Q = \frac{\mu_1 - \mu_0}{\sigma_1 - \sigma_0}$$

Where  $\mu_0, \mu_1, \sigma_1, \sigma_0$  are mean values and standard deviations of the 'one' and 'zero' measured just before the decision circuit of the receiver.

In this simulator, three different methods of BER estimation are used: Monte Carlo, semi-analytic and analytic, which will be explained in the following points.

## 4.2. Estimation methods

### 4.2.1. Monte Carlo

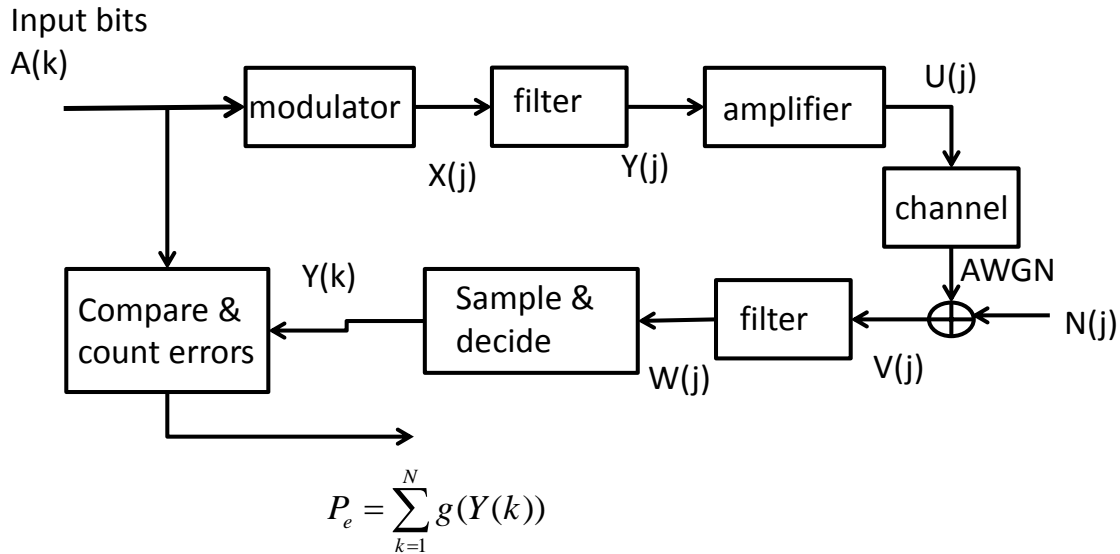


Figure 4.2-1. Monte Carlo estimator [8]

There are many variations of the Monte Carlo technique; it basically involves the simulation of a random experiment using artificial means.

In the context of the specific example shown in Figure 4.2-1. Monte Carlo estimator, Monte Carlo simulation for estimating the bit error rate in a digital communication system involves the following steps.

1. Generate sampled values of the input sequence,  $A(k)$ ; and the noise samples  $N(j)$ .
2. Process these samples through the models of the functional blocks and generate output sequence  $Y(k)$ .
3. Estimate  $E(g(Y(k)))$  as

Eq. 4.2-1

$$P_e = \sum_{k=1}^N g(Y(k))$$

Where  $g(Y(k)) = 1$  if  $Y(k) \neq A(k)$  and  $g(Y(k)) = 0$  if  $Y(k) = A(k)$ . This step is equivalent to counting errors.

### 4.2.2. Analytic

It is also referred to as deterministic analysis. The analytic method treats the signal waveforms and the noise samples separately. So, is necessary to construct a model where the signal samples are never corrupted by random noise samples. This means that all the optical elements in the simulation system must be configured to not add noise, and the noise samples have to be generated and propagated separately.

Then, the deterministic estimator is able to calculate the BER estimate by combining the results of the analysis of the signal waveform with the noise power calculated from the noise samples.

The main advantage of this kind of estimator is that the results do not depend upon random generated noise samples during a specific simulation run, and therefore good, stable estimates of BER can usually be obtained from a comparatively small number of bits.

On the other hand, the main disadvantage of deterministic estimation is that keeping the signal separated from the noise excludes the nonlinear interactions between signals and noise, and so there is a loss of accuracy.

As the mean and standard deviation parameters for the signal waveform are well known, either for the 'ones' and the 'zeros', the Q factor can be calculated, and then the BER estimation can be expressed as:

**Eq. 4.2-2**

$$BER = \frac{1}{n} \frac{1}{2} \operatorname{erfc} \left( \frac{Q}{\sqrt{2}} \right)$$

### 4.2.3. Semi-Analytic

In many cases, important nonlinear processes that are the result of the interactions between the signal and the noise –and affect noise statistics- occur mainly during the transmission and in the detection process.

If a Gaussian model; whose properties are easy to understand and very well known, is used for the noise added after the photodetection, the semi-analytic method is appropriate.

In the semi-deterministic method, all optical noise is accounted for in the form of noise samples added to the signal but all the post-detection electrical noise is still estimated using a deterministic model.

$$BER = \frac{1}{n} \sum_{i=1}^n \frac{1}{2} \operatorname{erfc} \left( \frac{Q_i}{\sqrt{2}} \right)$$

Where  $Q_i$  is the quality factor for each bit.

# Chapter 5 Simulation Examples

## 5.1.Simulation 1

In this simulation a non-dispersive scenario will be considered, and some performance parameters and diagrams will be obtained for the three modulations studied within the scope of the project.

For this first simulation, the following parameters will be used:

- Symbol Rate = 10.7e9
- Lambda = 1.55e-6
- Samples per bit= 128
- Numberof bits=1024
- SignalPower=1mw (0 dBm)
- Noise power= -60 dBm

Next we are going to obtain, for OOK, BPSK and QPSK, respectively, the following information:

- Information bits
- Modulated signal's module
- Demodulated signal's module
- Eye diagram

### OOK-NRZ

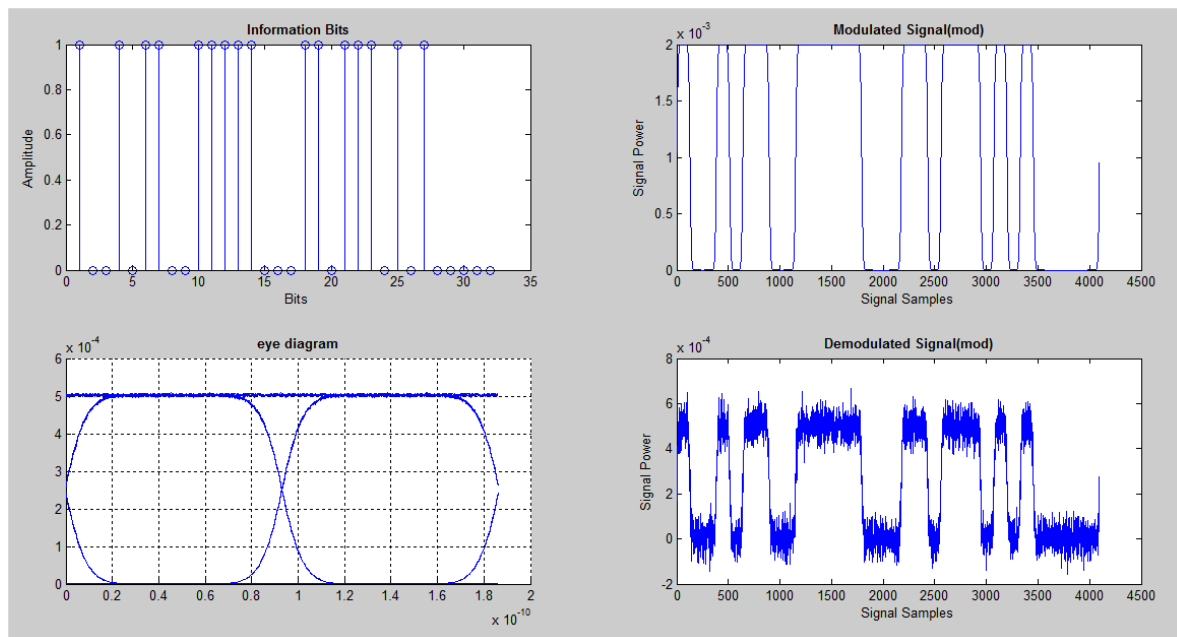


Figure 5.1-1.OOK simulation results



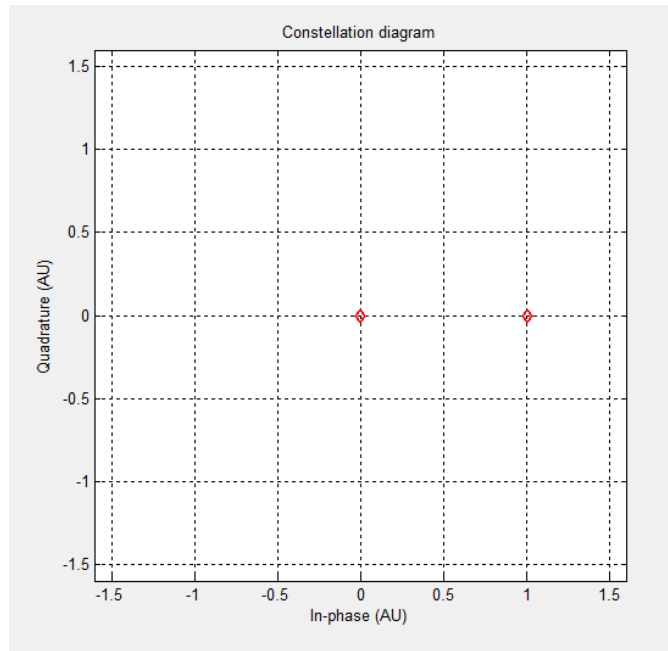


Figure 5.1-2. OOK constellation diagram

**BPSK**

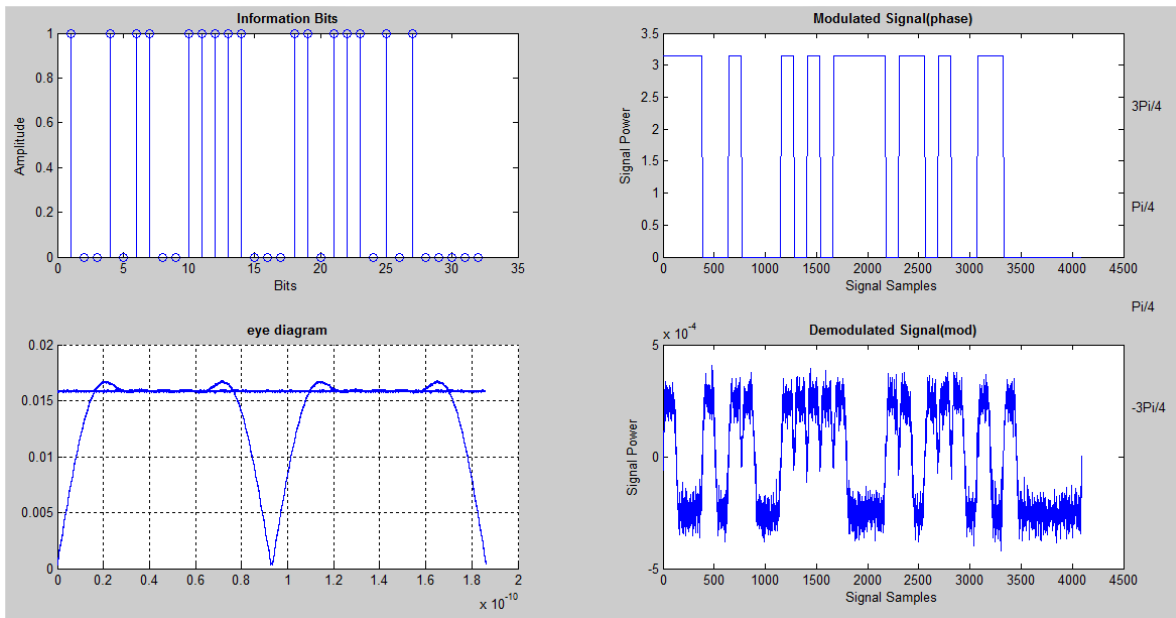


Figure 5.1-3.Simulation results BPSK

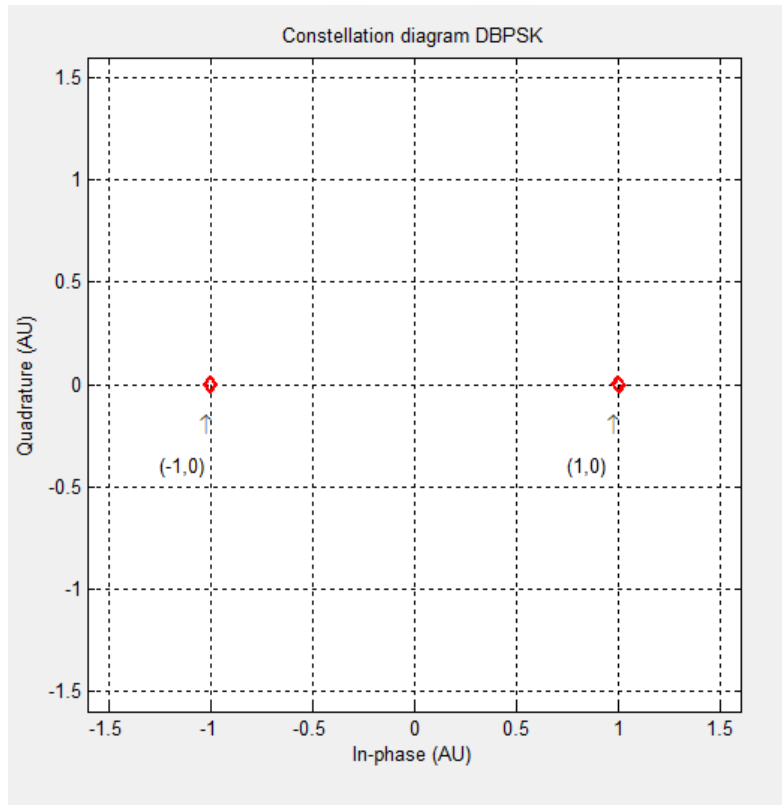


Figure 5.1-4. Constellation diagram BPSK

**DQPSK**

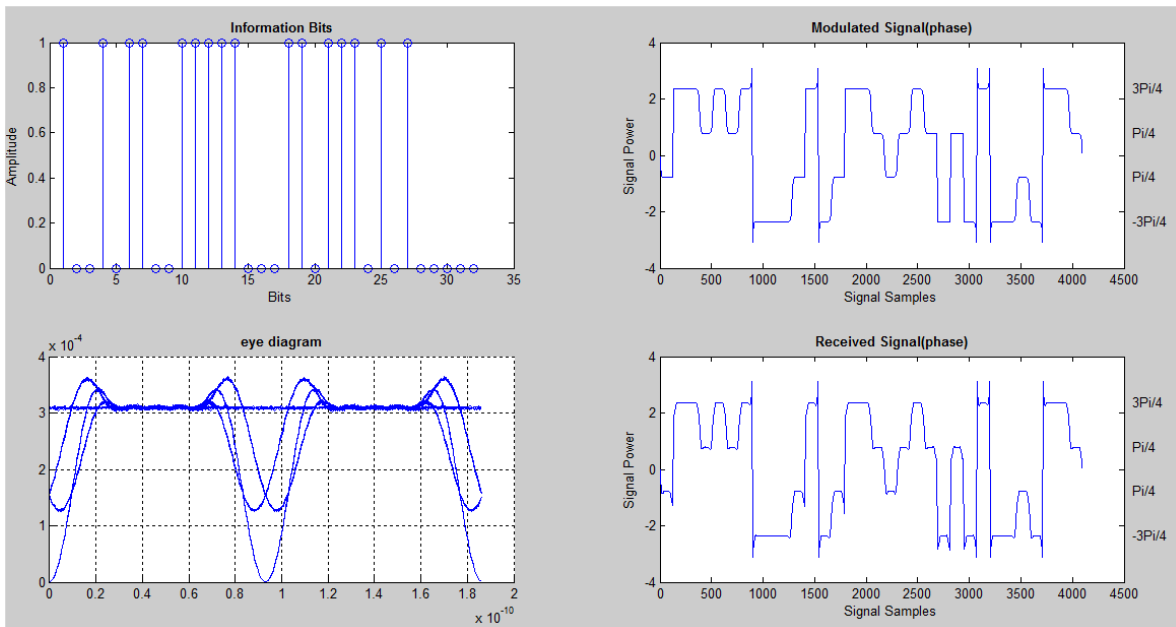


Figure 5.1-5. Simulation results DQPSK

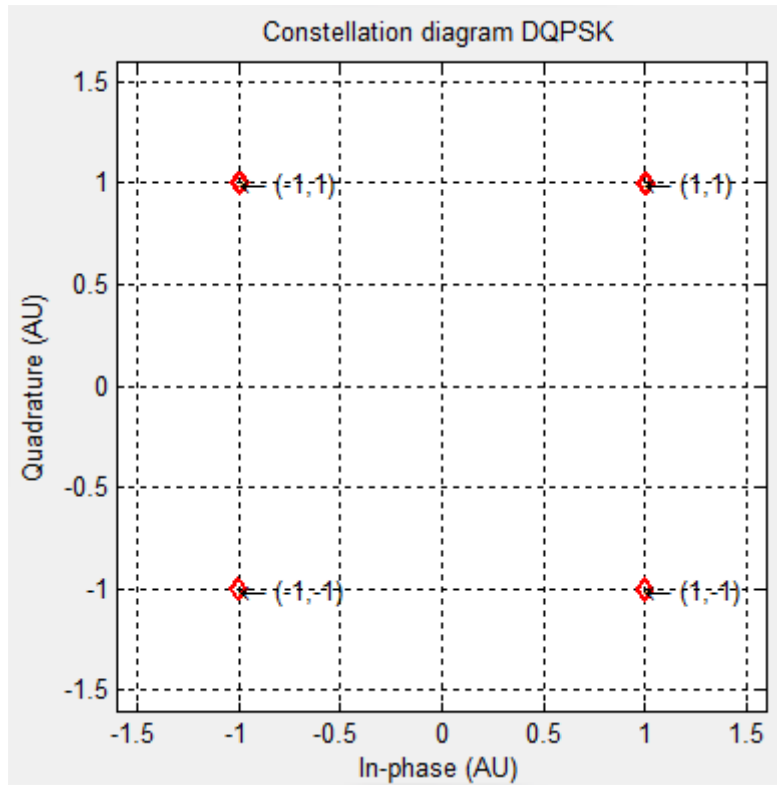


Figure 5.1-6. Constellation diagram DQPSK

## 5.2.Simulation 2

For the next simulation, the goal will be to obtain the receiver's sensitivity. In order to achieve that, the procedure will be putting a signal attenuator just before the detector until a BER of  $10^{-3}$  is obtained.

So, the value of signal power for which a BER of  $10^{-3}$  is achieved is in fact the desired receiver's sensitivity. In this case, the signal reference power is 0 dBm, and the main parameters used are:

- Symbol Rate = 10.7e9
- Lambda = 1.55e-6
- Samples per bit= 128
- Numberof bits=1024
- Noise power: -50 dBm

With this scenario, it is possible to plot the BER depending on the signal power, and the red line shows the reference BER chosen. The graphics are represented in a logarithmic scale for simplicity.

### OOK

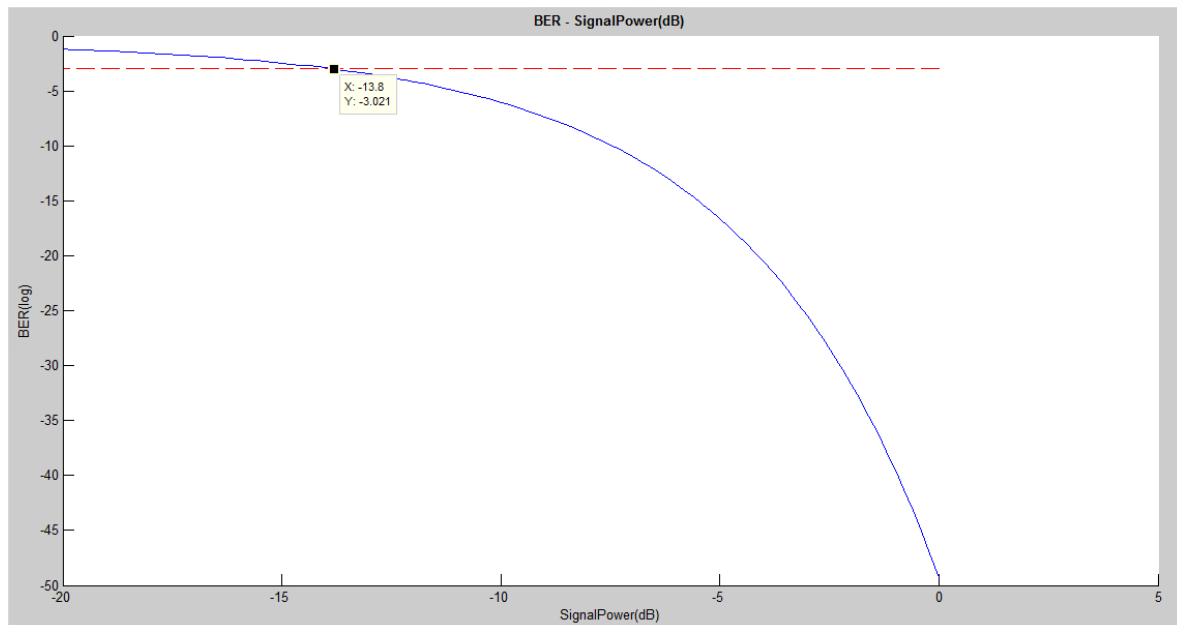


Figure 5.2-1. BER-Signal power(dB) - OOK

Sensitivity: -13.8 dBm

### DBPSK

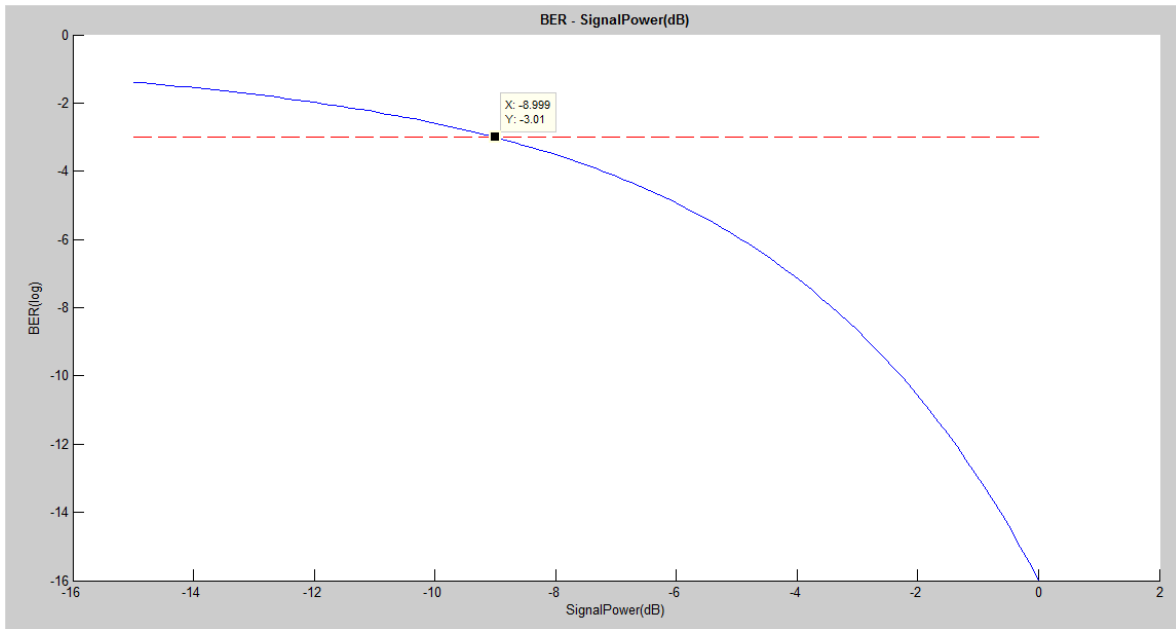


Figure 5.2-2 BER-Signal power(dB) -DBPSK

Sensitivity: -9 dBm

### DQPSK

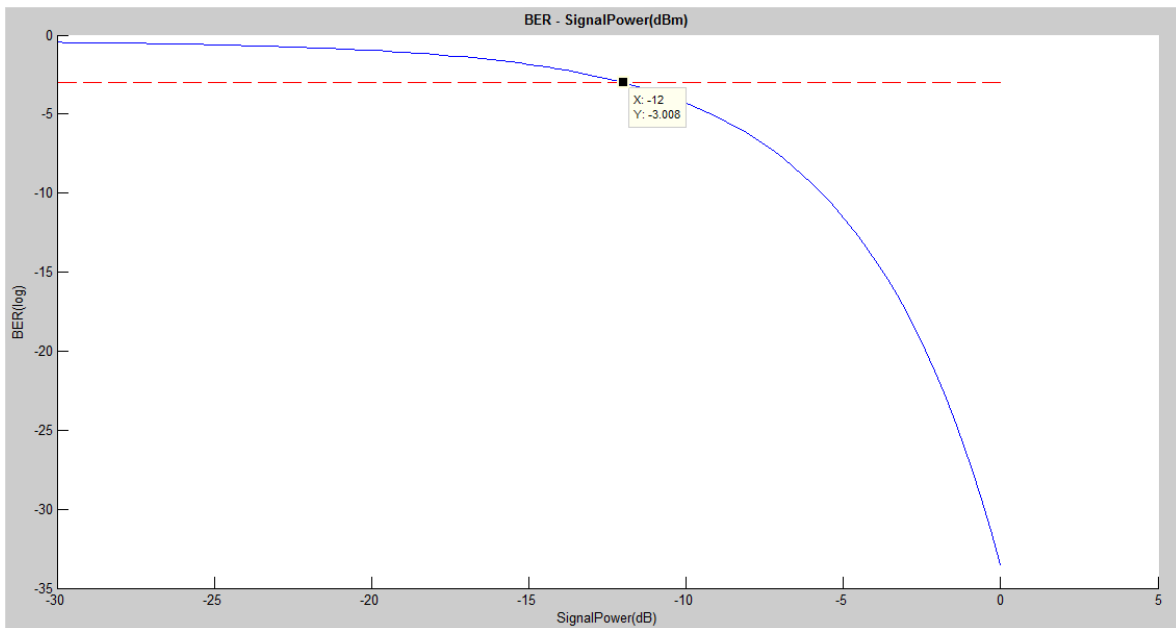


Figure 5.2-3. BER-Signal power(dB) -DQPSK

Sensitivity: -12 dBm

## 5.3. Simulation 3

The purpose of the third simulation is noticing the impact of the optical fiber dispersion on the received signal. Next, we can see both eye and constellation diagram for different values of the dispersion parameter ( $D$ ) in  $\text{ps}/\text{Km}\cdot\text{nm}$ .

Main parameters used:

- Symbol Rate =  $10.7\text{e}9$
- $\lambda = 1.55\text{e}-6$
- Samples per bit = 128
- Number of bits = 1024
- Noise power: -50 dBm

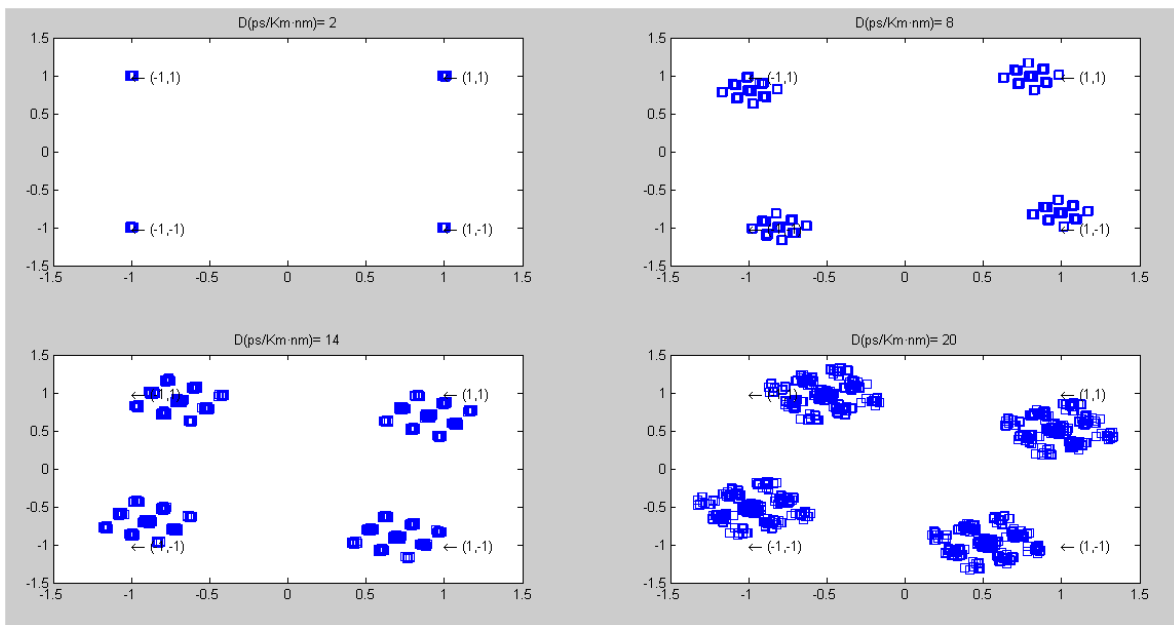


Figure 5.3-1. Constellation diagram evolution

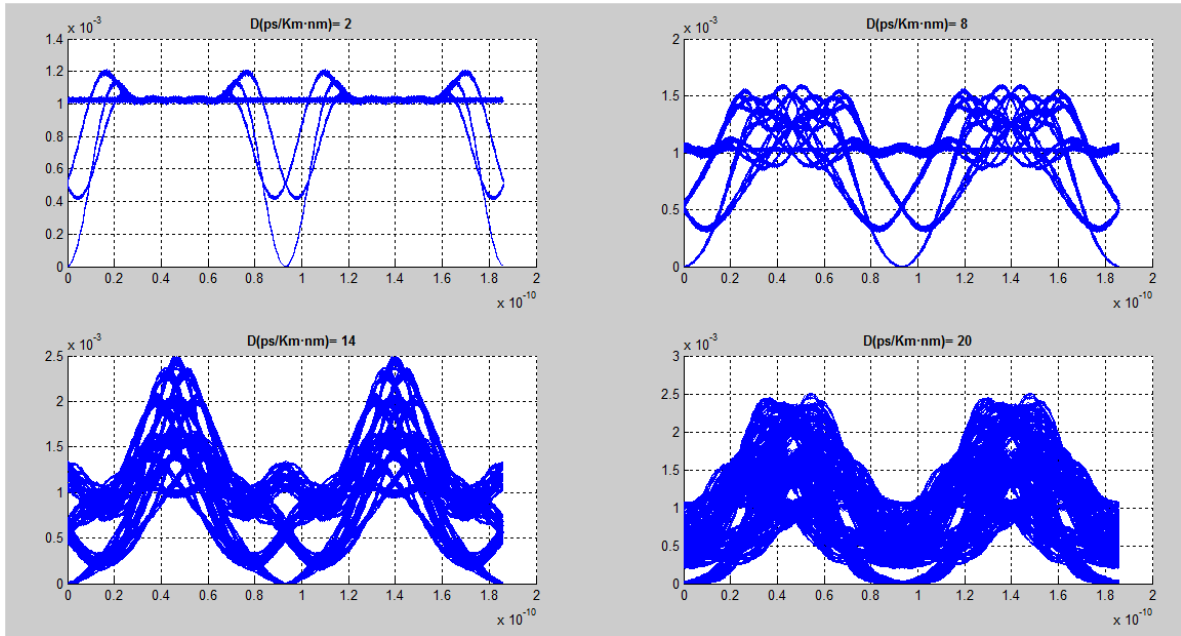


Figure 5.3-2. Eye diagram evolution

## References

- [1] E. Collett, *Field Guide to Polarization*, Bellingham: SPIE Press, 2005.
- [2] G. P. Agrawal, *Fiber-Optic communication systems*, New York: John Wiley and Sons, Inc. , 2002.
- [3] J. M. Gené, “Apunts Com. Òptiques,” Barcelona, 2011.
- [4] “RP photonics,” [Online]. Available: [http://www.rp-photonics.com/electro\\_optic\\_modulators.html](http://www.rp-photonics.com/electro_optic_modulators.html). [Accessed 07 octubre 2012].
- [5] M. Seimetz, in *High-Order Modulation for Optical Fiber Transmission*, Springer, 2009, p. 20.
- [6] I. Glover and P. Grant, *Digital Communications (2nd ed.)*, Pearson Education Ltd, 2004.
- [7] “wikipedia,” [Online]. Available: [http://en.wikipedia.org/wiki/Raised-cosine\\_filter](http://en.wikipedia.org/wiki/Raised-cosine_filter). [Accessed 06 octubre 2012].
- [8] Jeruchim, in *Simulation of communication systems -2nd edition*, 200, pp. 371-374.
- [9] “wikipedia,” [Online]. Available: <http://en.wikipedia.org/wiki/Photodiode>. [Accessed 16 september 2012].